Supplementary information

3D vs. turborstratic: controlling metal-organic framework dimensionality via N-heterocyclic carbene chemistry

Ilia Kochetygov,[a] Anita Justin,[a] Mehrdad Asgari,[a,b] Shuliang Yang,[a,c] Vikram Karve,[a] Till Schertenleib,[a] Dragos Stoian,[d] Emad Oveisi,[e] Mounir Mensi,[a] Wendy L. Queen*[a]

[a] Institute of Chemical Sciences and Engineering, École Polytechnique Fédérale de Lausanne (EPFL), CH-1951 Sion, Switzerland. E-mail: wendy.queen@epfl.ch

[b] Department of Chemical Engineering & Biotechnology, University of Cambridge, Philippa Fawcett Drive, Cambridge CB3 0AS, UK

[c] College of Energy, Xiamen University, Xiamen, Fujian, 361102, China

[d] Swiss–Norwegian Beamlines, ESRF, BP 220, Grenoble, 38043, France

[e] Interdisciplinary Centre for Electron Microscopy (CIME), École Polytechnique Fédérale de Lausanne (EPFL), CH-1015 Lausanne, Switzerland

1. General notes

Materials:

All the commercially available chemicals were used as received without further purification. $Cu(BF_4)_2 \cdot 6H_2O$ (99 %) and n-octane (>99 %) were obtained from ABCR, $CDCl_3$ (>99.8 % D) was obtained from Acros, ethanol (A15 pharmaceutical grade) was obtained from Reactolab SA, anhydrous tetrahydrofuran (THF, >99.5 %) and trans-stilbene (>98.0 %) were obtained from TCI, $[Ir(cod)(OMe)]_2$ was obtained from Sigma-Aldrich (cat. #685062), anhydrous toluene (≥99.5 %), HNO_3 (69 %), HCl (37 %), ICP elemental standards for B and Cu were obtained from Carl Roth AG, Ir ICP elemental standard was obtained from Alfa Aesar.

X-Ray crystallography:

Laboratory single-crystal X-ray diffraction was performed at 100 K using a Bruker D8 Venture diffractometer equipped with a graphite monochromator and microfocused MoKα radiation source

(λ = 0.71073 Å). The data was integrated with SAINT[1] and corrected for adsorption with SADABS software. [2] Synchrotron single crystal and powder X-ray diffraction data were collected using a multipurpose PILATUS@SNBL diffractometer with PILATUS 2M detector at the BM01 at European Synchrotron Radiation Facility (λ = 0.6866 Å). Single crystals were mounted on a Kapton loop and measured at 100 K. The structure solution and refinement were performed using ShelXT[3] and ShelXL-2013[4] operated through the Olex2 interface.[5] First, non-hydrogen atoms were located and refined anisotropically, then H atoms were introduced with corresponding HFIX commands and refined isotropically. Powders were loaded in 1mm diameter glass capillaries and measured at 300 K in ambient conditions for *ex situ* samples. For studies of *in situ* material activation, the MOF sample was loaded in a capillary connected to a custom-built manifold and evacuated using a turbomolecular pump ($< 10^{-2}$ mbar). Then, a temperature ramp was applied and the material was heated to 190 °C over 90 minutes, kept at that temperature for 20 minutes, and cooled down to room temperature over 50 minutes. The sample structure evolution was followed by measuring a powder pattern each minute. The data was visualized using MEDVED software. [6] Laboratory powder X-ray diffraction was performed using Bruker D8 Discover instrument equipped with Cu Kα radiation source operated in Bragg–Brentano geometry. The scan step was 0.02 ° and the time per step was 1 s.

FTIR measurements

The *in situ* FTIR data was collected using a PerkinElmer FTIR/FIR spectrometer. Ca. 20 mg of sample was mixed with ca. 200 mg of KBr and placed into a custom-built cell with diffuse reflectance Praying Mantis™ accessory. The sample was first activated by heating at 185 °C in vacuum for 15 h. Then the sample was cooled to −123 °C (150 K) and dosed with selected CO pressures using a custom-built gas manifold. The spectra were collected at 1 cm^{-1} resolution. All spectra were background-subtracted.

TGA

Thermogravimetric analysis (TGA) and decomposition temperatures were determined from TGA experiments on a TGA Q500 device from TA Instruments in 100 µl platinum pans with an empty pan of the same type as reference.

ICP

An exact amount of ca. 10 mg of MOF material was digested, inside a PTFE vial, in 1 mL of aqua regia (1:3 v/v HNO_3 69 %+HCl 37 %) at 100 °C for 1h and further overnight at room temperature. The solution was diluted to 25 mL in a volumetric flask using 2 % HCl as a matrix, filtered through 0.22 μm syringe membrane filter and analyzed via ICP-OES using Agilent 5110 instrument. The averaged element concentrations and their standard deviations were extracted using 5 chosen, most intense and non-overlapping wavelengths.

NMR

Solution NMR spectra were recorded in $CDCl_3$ using a BRUKER AVIII HD 400 spectrometer; chemical shift values were referenced to 1 % TMS solution in $CDCl_3$ using the residual solvent signals as a secondary reference. Digestion NMR was performed in a mixture of D_2SO_4 (66 uL) and DMSO-d6 (600 uL). The MOF was sonicated in this mixture until no solid was present. The Bruker Topspin software package (version 3.2) was used for measurements and Mestrenova software (version 12.0.0-20080) was used for processing of the spectra.

Solid-state ^{13}C NMR was performed at room temperature using a 500 MHz 3.2 mm LTMAS probe at 24 kHz MAS, with an Avance III Bruker console.

Electron microscopy

SEM images were acquired on a Thermo Scientific Teneo SEM instrument using an ETD detector at an accelerating voltage of 2.0 kV. Bright-field transmission electron microscopy (TEM) images were taken using the Thermo Scientific Tecnai G2 Spirit Twin instrument at an accelerating voltage of 120 kV. High-angle annular dark-field scanning transmission electron microscopy (HAADF-STEM) imaging was performed on a double Cs-corrected Thermo Scientific Titan Themis instrument operated in scanning mode at an accelerating voltage of 200 kV. This microscope is equipped with a high brightness X-FEG gun and four silicon drift Super-X EDX detectors.

X-ray photoelectron spectroscopy (XPS)

XPS measurements were carried out using a Kratos AXIS Supra spectrometer with an Al Kα X-ray source. All measurements are done with an emission current of 15 mA and all data was collected with a pass energy of 40 eV and a step size of 0.1 eV. All binding energies were calibrated with respect to the C-C (C 1s) bond at 284.8 eV. Elemental fitting was done using ESCApe software by Kratos Analytical. All spectra were fit using a convolution of Gaussian and Lorentzian line shapes with a ratio of 70:30. A splitting of 3.0 eV with a ratio of 4:3 was used for the spin-orbit coupling of Ir 4f5/2 and 4f7/2 and a fixed FWHM was used. For metallic Ir, asymmetric line shape with an asymmetry of 0.5 was used.

X-ray absorption spectroscopy (XAS)

XAS spectra on Ir L_{III} absorption edges were acquired on an SNBL BM31 beamline of ESRF, Grenoble, France in transmission mode using two ionization chambers as detectors. The SNBL is equipped with a Si(111) double crystal monochromator for EXAFS data collection. The data was measured with a step size of 0.5 eV. Three reference materials, Ir metal (as a foil), $[Ir(cod)(OMe)]_2$ and $Ir(acac)_3$ (acac stands for acetylacetonate ligand) were measured in addition to the two samples. $[Ir(cod)(OMe)]_2$ and $Ir(acac)_3$ were diluted with cellulose prior to measurement, while other materials were measured neat.

2. Synthetic protocols

H_2Sp5-BF_4 and **Cu-Sp5** were synthesized and characterized as previously described.[7]

Cu-Sp5-BF_4 large-scale synthesis. In a 500 mL Schott bottle, 1.761 g of $Cu(BF_4)_2\cdot 6H_2O$ (5.100 mmol) was dissolved in 167 mL of ethanol. To this solution was added 1.435 g (3.604 mmol) of finely ground H_2Sp5-BF_4 and the mixture was sonicated for 10 minutes to form a well-dispersed pale blue slurry. The bottle was transferred into a temperature-programmed oven and the following program was applied: ramp to 80 °C over 8 h, stay at 80 °C for 72 h, turn off heating, and cool naturally inside the oven. The pale blue crystals were filtered on a G3 frit and washed with ethanol until the filtrate was clear and colorless. The material was further dried in vacuum (10^{-2} mbar) to produce **Cu-Sp5-BF_4-EtOH**. Anal. Calcd for $Cu(C_{17}H_{13}N_2O_4)(BF_4)(C_2H_5OH)_{1.6}(H_2O)_{0.6}$: C, 44.59; H, 4.41; N, 5.15. Found: C, 44.65; H, 4.41; N, 5.17.

Cu-Sp5-BF_4 single crystal synthesis. In a 8 ml vial, 10.3mg (0.03 mmol) of $Cu(BF_4)_2\cdot 6H_2O$ was dissolved in 3 mL of ethanol. To this was added 12 mg (0.03 mmol) of finely ground H_2Sp5-BF_4.

The mixture was sonicated for 10 minutes and transferred into a temperature-programmed oven and the following program was applied: ramp to 80 °C over 8 h, stay at 80 °C for 48 h, ramp to 25 °C during 8 h. The blue crystals were washed with ethanol by decantation until the supernatant was clear and colorless. The material was further dried in vacuum (10^{-2} mbar) to produce **Cu-Sp5-BF$_4$-EtOH**. Anal. Calcd for $Cu(C_{17}H_{13}N_2O_4)(BF_4)(C_2H_5OH)_{1.6}(H_2O)_{0.7}$: C, 44.44; H, 4.43; N, 5.13. Found: C, 44.52; H, 4.28; N, 4.93.

Cu-Sp5-BF$_4$ activation. In a 20 mL vial equipped with a septum cap, vacuum-dried pale blue **Cu-Sp5-BF$_4$·solvent** was placed and connected to a vacuum line via needle. The vial was heated stepwise in an oil bath (80 °C → 120 °C →160 °C → 185 °C), staying for 1 h at each intermediate temperature, and kept at 185 °C overnight. The resulting dark green crystals of **Cu-Sp5-BF$_4$-A** were cooled down under vacuum, dosed with N_2 from the Schlenk line, and immediately transferred to a nitrogen-filled glove box. Anal. Calcd for $Cu(C_{17}H_{13}N_2O_4)(BF_4)$: C, 44.42; H, 2.85; N, 6.09. Found: C, 44.06; H, 2.08; N, 5.58. B:Cu molar ratio (ICP): 1.02(3):1.

Cu-Sp5-OMe synthesis. In a nitrogen-filled glovebox, 1.000 g of **Cu-Sp5-BF$_4$-A** (2.176 mmol) was added to a solution of 123.5 mg sodium methoxide (2.286 mmol, 1.05 eq) in 300 mL anhydrous methanol in a 1L Schott bottle. The bottle was tightly capped and placed on a magnetic stirrer plate at 300 rpm speed. After stirring for 24 h under nitrogen at room temperature, the mixture was allowed to stand still for 30 minutes and most of the liquid was decanted. The solid was isolated using centrifugation (3 min, 6000 rpm) and washed 3 times with 100 mL methanol. The obtained material, **Cu-Sp5-OMe,** was vacuum dried and then activated at 120 °C in vacuum overnight to produce **Cu-Sp5-OMe-A**. Anal. Calcd for $Cu(C_{17}H_{13}N_2O_4)(BF_4)_{0.22}(OCH_3)_{0.78}(H_2O)_{2.4}$: C, 46.49; H, 4.42; N, 6.10. Found: C, 46.15; H, 4.33; N, 6.14. B:Cu molar ratio (ICP): 0.22(2):1.

Cu-Sp5-BF$_4$-A methanol treatment.

100 mg of **Cu-Sp5-BF$_4$-A** was placed in 30 mL of anhydrous methanol and stirred at 300 rpm speed under N_2 for 24 hours. The resulting material was isolated using centrifugation (3 min, 6000 rpm) and washed 3 times with 30 mL methanol. B:Cu molar ratio (ICP): 1.01(2):1.

Cu-Sp5-OMe synthesis with 1.5 eq of MeONa. In a nitrogen-filled glovebox, 0.1 g of **Cu-Sp5-BF$_4$-A** (0.2176 mmol) was added to a solution of 17.6 mg sodium methoxide (0.3258 mmol, 1.5 eq) in 30 mL anhydrous methanol in a 40 mL vial. The vial was tightly capped and stirred at 300 rpm speed. After stirring for 24 h under nitrogen at room temperature, the solid was isolated using centrifugation (3 min, 6000 rpm) and washed 3 times with 30 mL methanol. B:Cu molar ratio (ICP): 0.049(6):1.

Cu-Sp5-OMe treatment with 0.2 eq of MeONa. In a nitrogen-filled glovebox, 0.1 g of **Cu-Sp5-OMe** (0.24 mmol) was added to a solution of 2.6 mg sodium methoxide (0.0.048 mmol, 0.2 eq) in 6 mL anhydrous methanol in a 20 mL vial. The vial was tightly capped and stirred at 300 rpm speed. After stirring for 24 h under nitrogen at room temperature, the solid was isolated using centrifugation (3 min, 6000 rpm) and washed 3 times with 30 mL methanol. B:Cu molar ratio (ICP): 0.053(3):1.

Iridium grafting procedure. In a nitrogen-filled glovebox, a solution of 252 mg [Ir(cod)(OMe)]$_2$ (0.380 mmol = 0.760 mmol Ir, 1 eq Ir) in 35 mL anhydrous THF was prepared in a 100 mL Schlenk flask. To this solution, 350 mg of either **Cu-Sp5-BF$_4$-A** (0.760 mmol) or **Cu-Sp5-OMe-A** (0.841 mmol) was added. The Schlenk flask was connected to a reflux condenser under nitrogen and the mixture was allowed to stir for 16 h at room temperature. After this soaking step, the mixture was heated to reflux (oil bath temperature 75 °C) for 24 h. Upon cooling, the mixture was separated using a centrifuge and the solid was washed with THF until the supernatant was colorless (5x50 mL). The materials were dried in vacuum overnight and stored in a nitrogen-filled glovebox, to produce **Ir/Cu-Sp5-BF$_4$-A** and **Ir/Cu-Sp5-OMe** accordingly. **Ir/Cu-Sp5-BF$_4$-A:** B:Cu ratio (ICP): 1.02(3):1. Ir(wt .%): 0.82(1). **Ir/Cu-Sp5-OMe:** B:Cu ratio (ICP): 0.23(1):1. Ir(wt .%): 2.47(6).

3. Catalysis protocols

Catalytic test protocol. In a nitrogen-filled glovebox, a stock solution of 2.143 g *trans*-stilbene and 0.676 g n-octane (internal standard) in anhydrous toluene was prepared in a 25 mL volumetric flask. 2.918 mL of this solution (corresponding to 0.250 g *trans*-stilbene, 1.387 mmol) was added into a Parr pressure vessel. To this solution, an amount of catalyst corresponding to 0.25 mol% Ir (25.6 mg for **Ir/MOF-OMe**, 77.4 mg for **Ir/MOF**) was added, the vessel was sealed and removed from the glovebox and subsequently pressurized with 5 bar H_2 after 3 purges. The reaction was run at 40 °C for 24 hours. To stop the reaction, the vessel was cooled down in an ice bath and subsequently depressurized. The solid catalyst was removed using centrifugation and washed with THF 3 times. It was later dried in vacuum and stored in the glovebox for further characterization and recycle test. The liquid toluene solution was analyzed using ^1H NMR in $CDCl_3$ to determine the yield and the conversion.

Split test protocol. A catalytic reaction was run as described above for a period of 2 hours instead of 24 hours. Afterward, upon stopping the reaction and centrifugation, the supernatant was additionally filtered using a 0.22 μm syringe membrane filter to ensure the removal of all the solid material. A sample of the solution was taken for ^1H NMR and the rest of it was loaded in the reactor again and the reaction was run for extra 20 hours as described above. Upon stopping the reaction, the solution was analyzed again using ^1H NMR spectroscopy.

Table S1. Crystallographic data for **Cu-Sp5-BF$_4$-EtOH** and **Cu-Sp5-BF$_4$-A**

Material	**Cu-Sp5-BF$_4$-EtOH**	**Cu-Sp5-BF$_4$-A**
Empirical formula	$C_{19}H_{14}BCuF_4N_2O_5$	$C_{17}H_{13}BCuF_4N_2O_4$
Formula weight	500.67	459.64
Temperature/K	100(2)	99.99
Crystal system	monoclinic	monoclinic
Space group	$P2_1/n$	$P2_1/c$
a/Å	6.6391(5)	14.932(3)
b/Å	33.5424(9)	31.562(5)
c/Å	11.4021(9)	14.861(3)
α/°	90	90
β/°	106.155(8)	98.450(6)
γ/°	90	90
Volume/Å^3	2438.9(3)	6928(2)
Z	4	12
ρ_{calc}g/cm^3	1.364	1.322
μ/mm^{-1}	0.873	0.999
F(000)	1008.0	2772.0
Crystal size/mm^3	0.15 × 0.03 × 0.03	0.1 × 0.02 × 0.02
Radiation	synchrotron (λ = 0.6866)	MoKα (λ = 0.71073)
2Θ range for data collection/°	3.78 to 65.1	1.29 to 46.848
Index ranges	$-6 \leq h \leq 6$, $-51 \leq k \leq 51$, $-17 \leq l \leq 17$	$-16 \leq h \leq 16$, $-35 \leq k \leq 35$, $-15 \leq l \leq 16$
Reflections collected	22331	79663
Independent reflections	5858 [R_{int} = 0.2689, R_{sigma} = 0.1810]	9973 [R_{int} = 0.1906, R_{sigma} = 0.1227]
Data/restraints/parameters	5858/3/345	9973/459/495
Goodness-of-fit on F^2	1.047	1.488
Final R indexes [I>=2σ (I)]	R_1 = 0.0779, wR_2 = 0.2260	R_1 = 0.1261, wR_2 = 0.3637
Final R indexes [all data]	R_1 = 0.0882, wR_2 = 0.2403	R_1 = 0.2099, wR_2 = 0.4251
Largest diff. peak/hole / e Å^{-3}	1.65/-1.54	1.86/-1.51

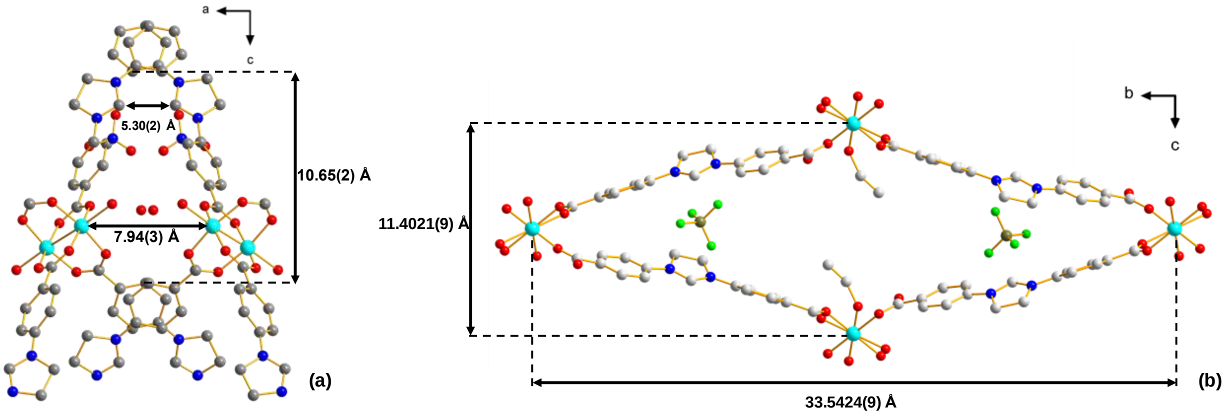

Figure S1. Comparison of (a) **Cu-Sp5-H_2O** and (b) **Cu-Sp5-BF_4-EtOH** structures

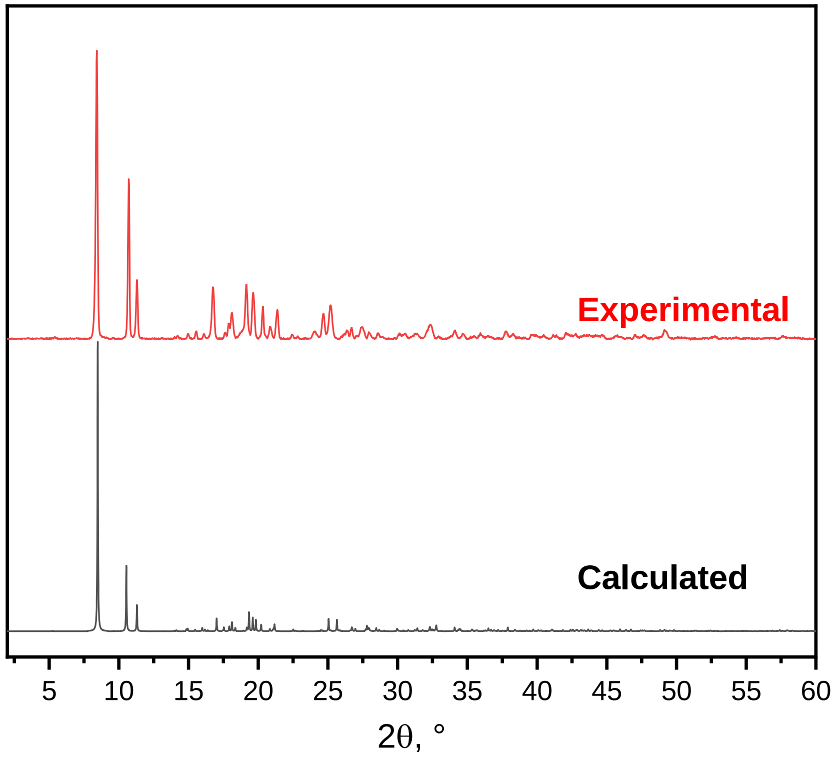

Figure S2. PXRD data for **Cu-Sp5-BF_4-EtOH**

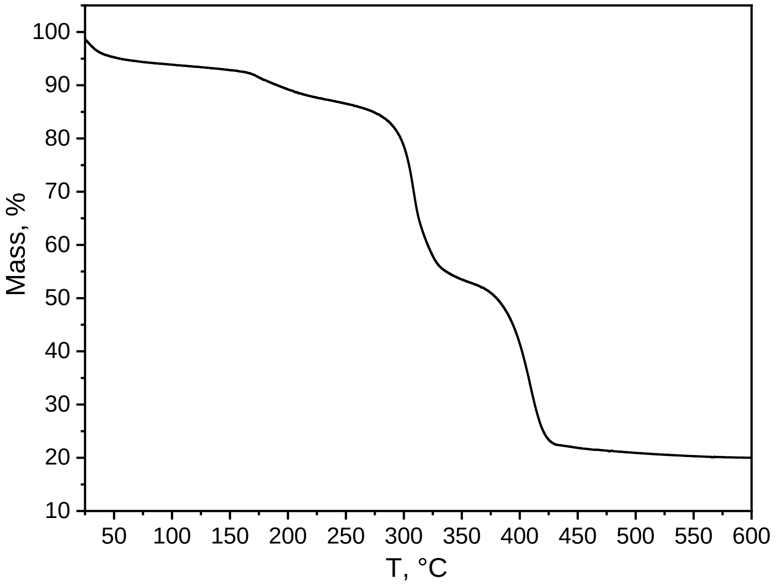

Figure S3. TGA curve for **Cu-Sp5-BF4-EtOH** (air, 5 °C/min)

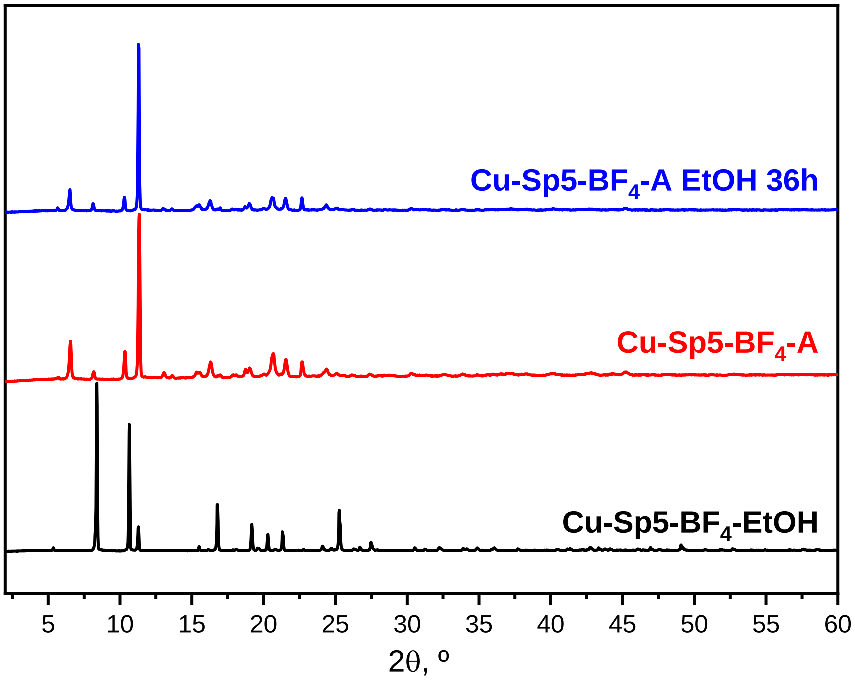

Figure S4. Comparison of PXRD patterns for **Cu-Sp5-BF4-EtOH** and **Cu-Sp5-BF4-A**

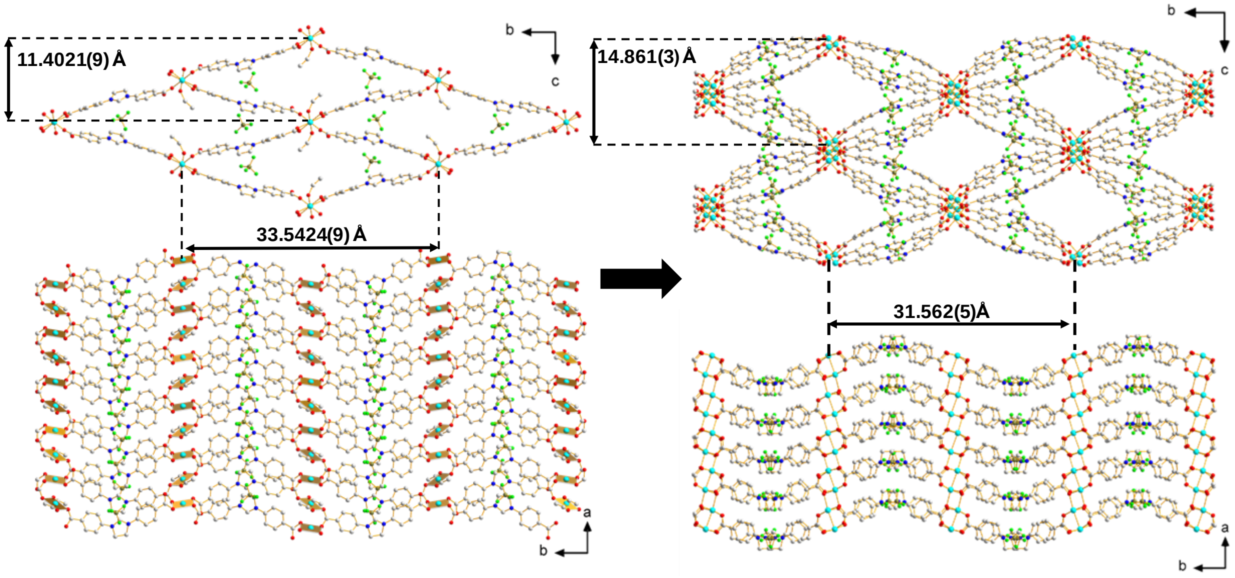

Figure S5. Structure of **Cu-Sp5-BF$_4$-EtOH** (left) and its activated counterpart, **Cu-Sp5-BF$_4$-A** (right), as viewed along the *a* axis (top) and the *c* axis (bottom). The number of Cu atoms along the *a* axis is the same in both pictures. Hydrogen atoms are omitted for clarity

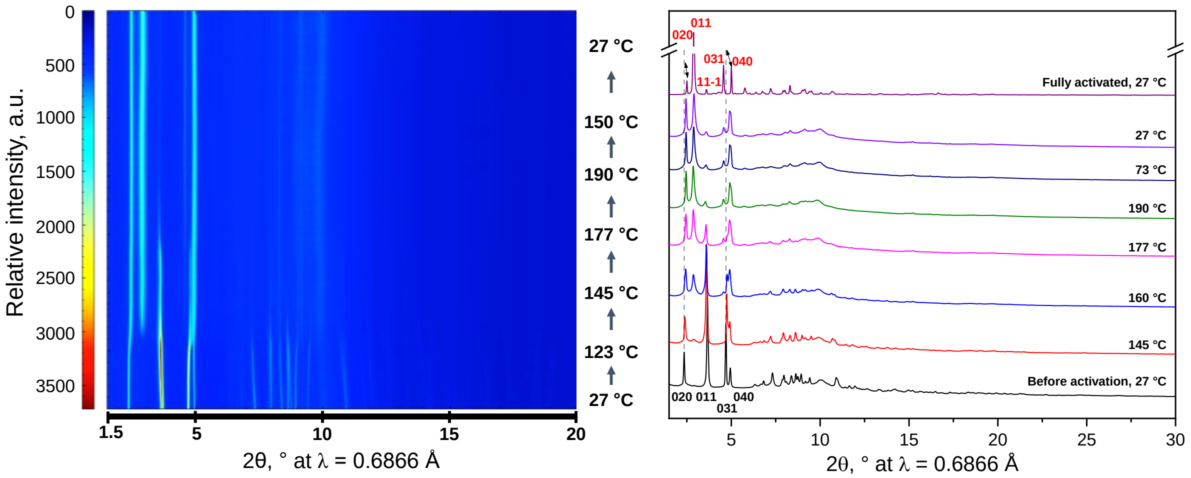

Figure S6. *In situ* PXRD data for **Cu-Sp5-BF$_4$** activation

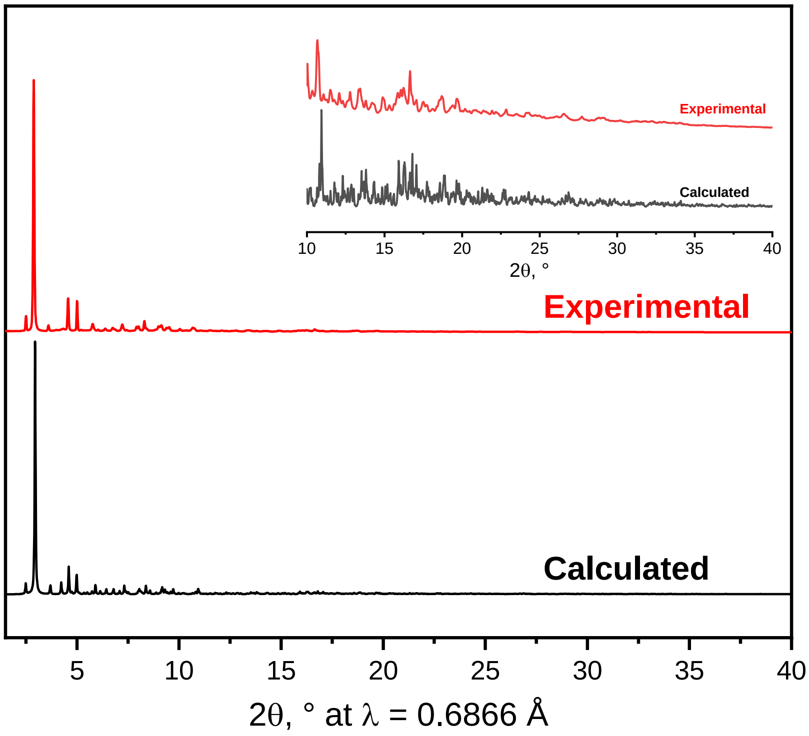

Figure S7. Synchrotron PXRD data for **Cu-Sp5-BF$_4$-A**

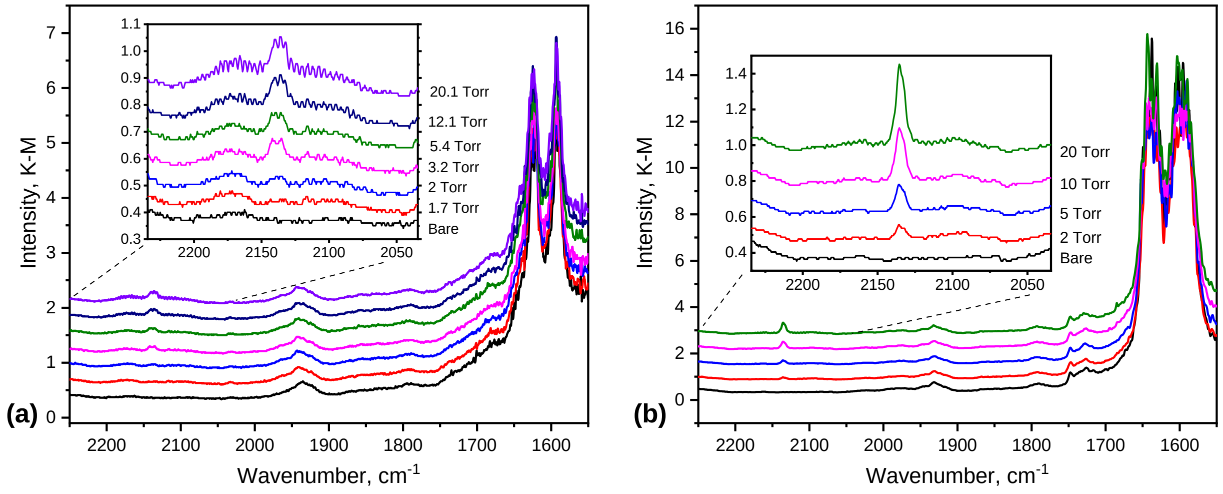

Figure S8. In situ DRIFTS spectra of (a) **Cu-Sp5-BF$_4$-A** and (b) **Cu-Sp5** upon CO dosage at 150 K

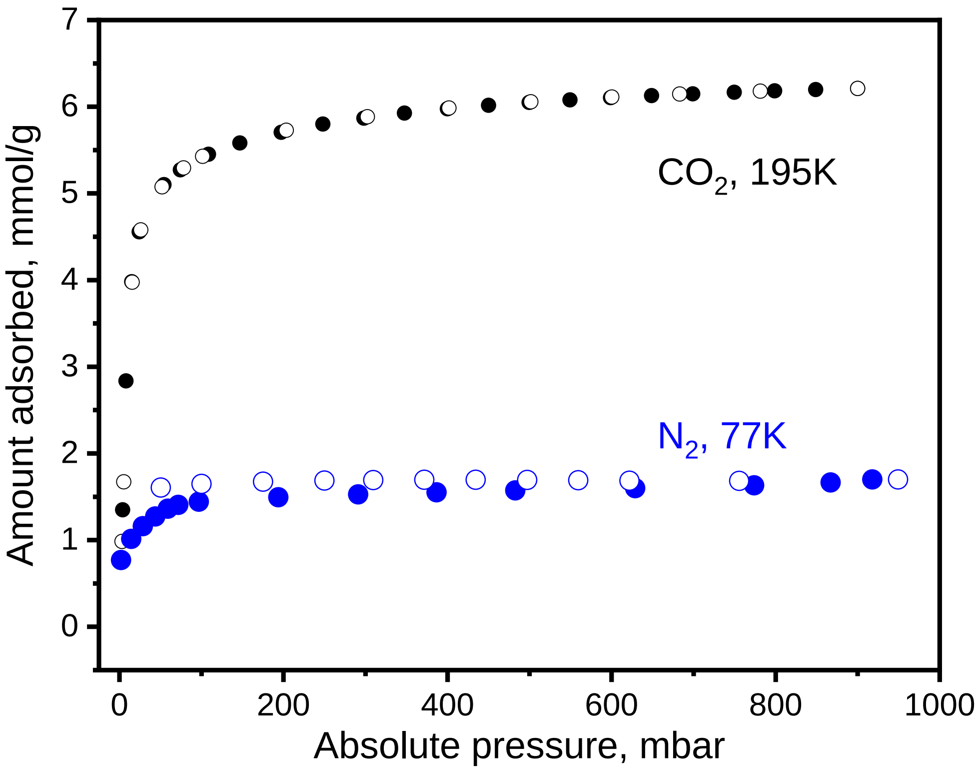

Figure S9. Gas adsorption isotherms (CO_2, 195 K and N_2, 77 K) for **Cu-Sp5-BF$_4$-A.** Closed symbols represent adsorption, open symbols represent desorption

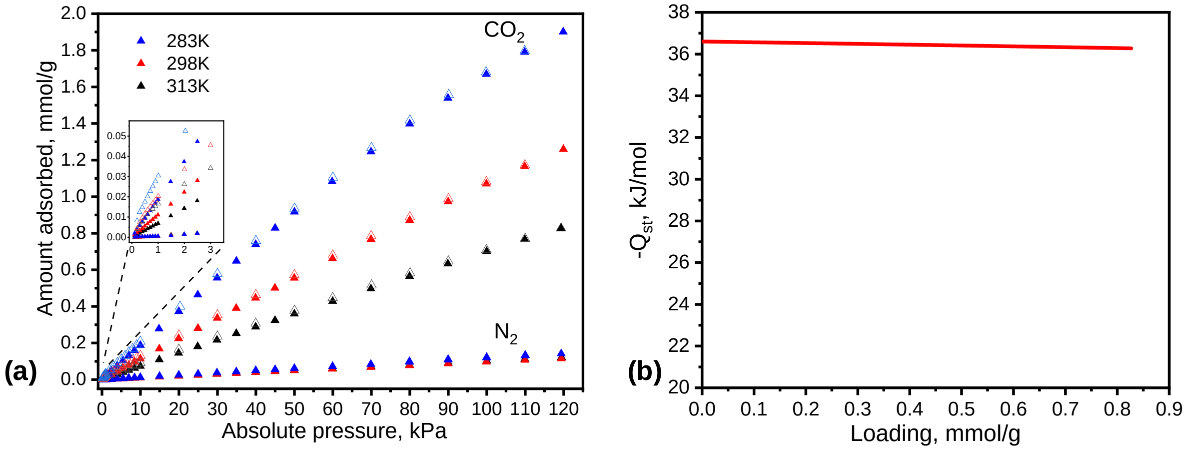

Figure S10. (a) Gas adsorption isotherms of CO_2 (top) and N_2 (bottom) for **Cu-Sp5-BF$_4$-A** at 283 K, 298 K, and 313 K (b) Isosteric heat of adsorption of CO_2 for **Cu-Sp5-BF$_4$-A**

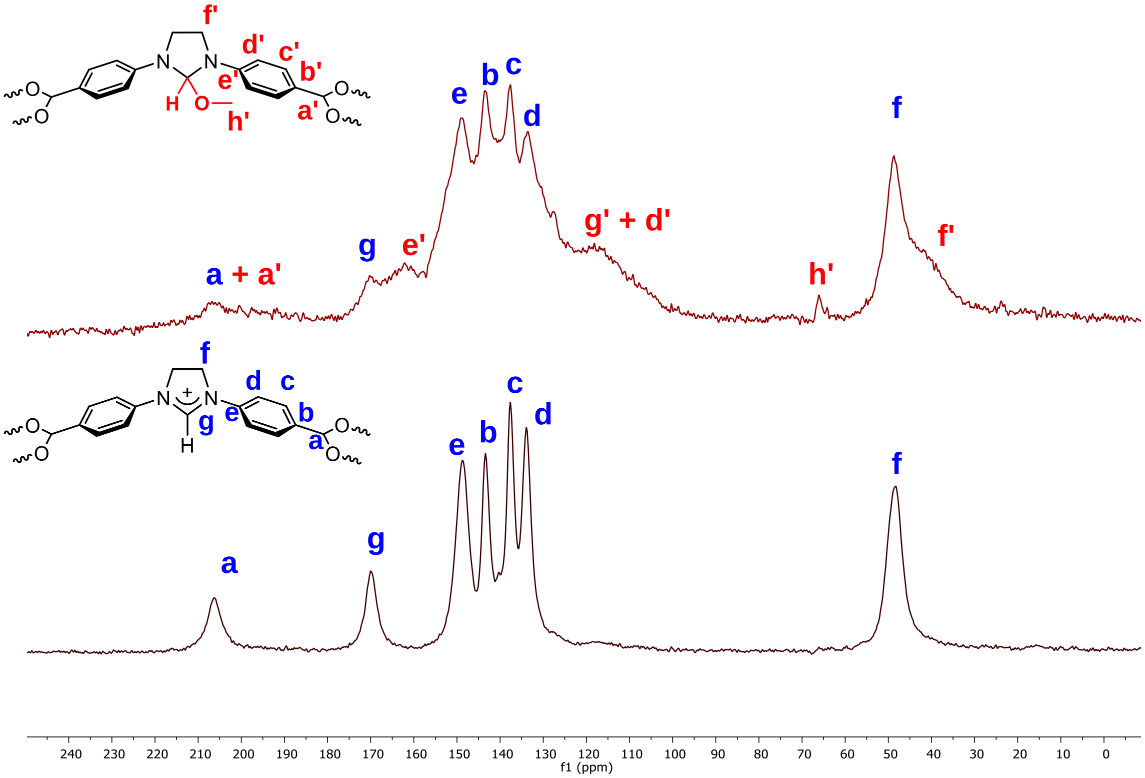

Figure S11. Solid-state ^{13}C MAS of **Cu-Sp5-BF$_4$-A** (bottom) and **Cu-Sp5-OMe** (top)

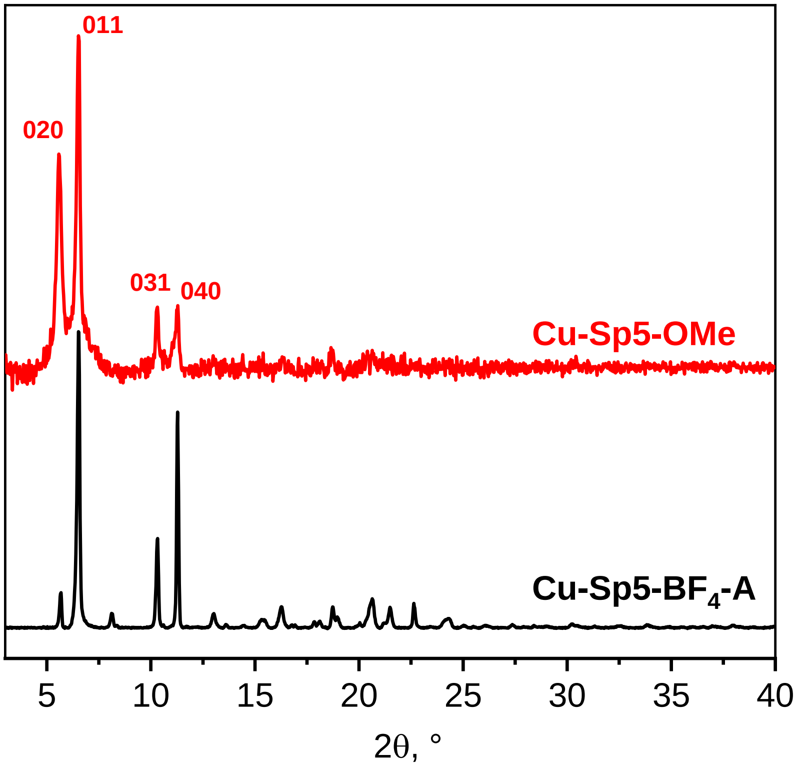

Figure S12. PXRD of **Cu-Sp5-OMe** and **Cu-Sp5-BF$_4$-A**

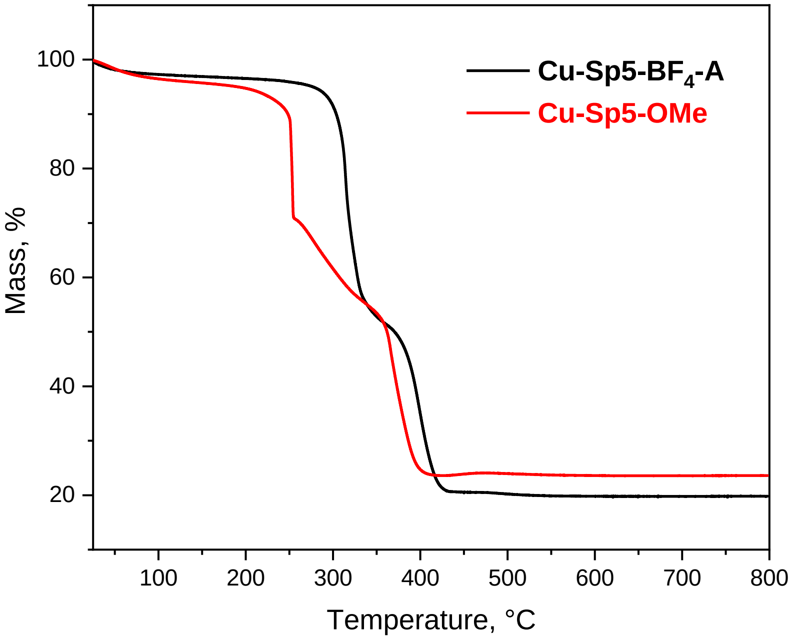

Figure S13. TGA curves of vacuum-dried **Cu-Sp5-OMe** and **Cu-Sp5-BF$_4$-A**

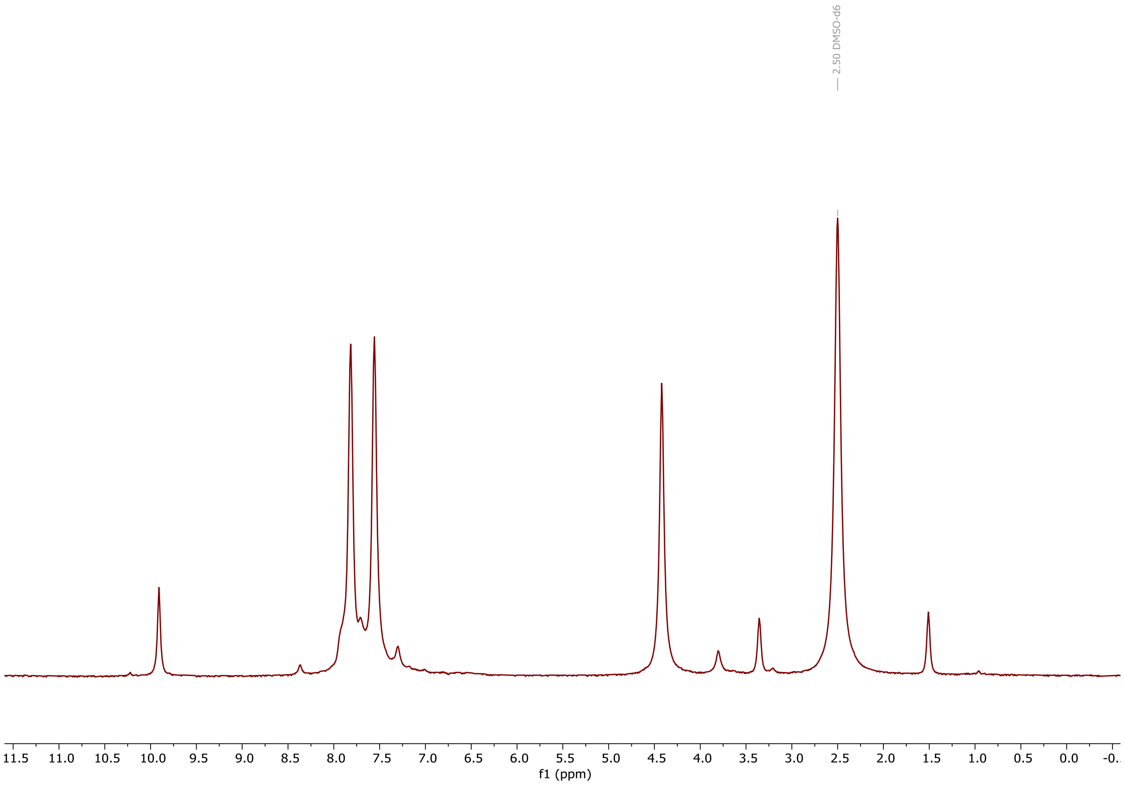

Figure S14. ^1H digestion NMR of vacuum-dried **Cu-Sp5-OMe** in DMSO-d6 + D_2SO_4

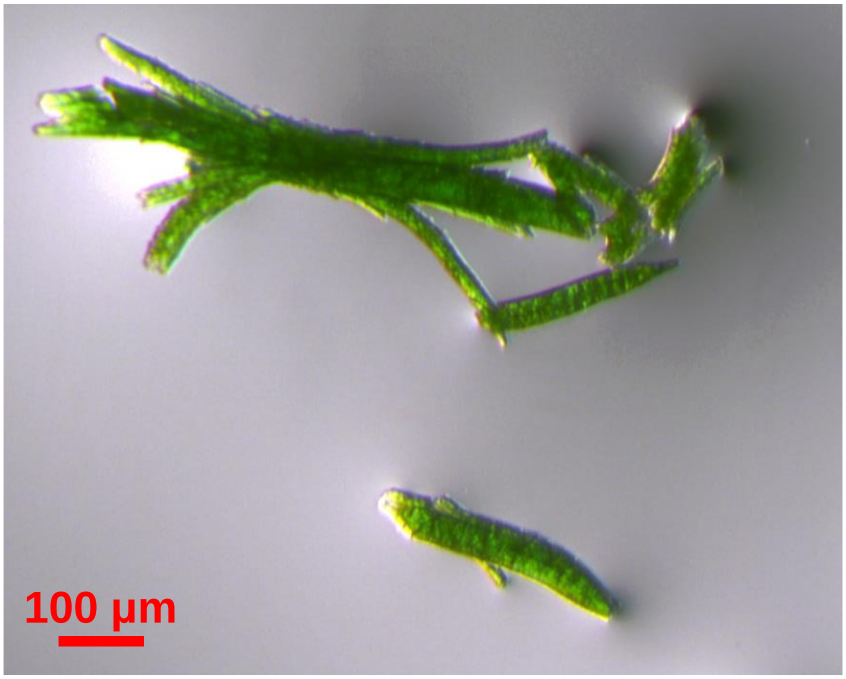

Figure S15. Light microscope image of **Cu-Sp5-OMe** particles

Unit Cell:

a= 6.62Å, α= 90.00°, V=2406Å³
b=33.47Å, β=106.69°, Monoclinic P
c=11.33Å, γ= 90.00°

Figure S16. A photo of **Cu-Sp5-BF4** crystal mounted on the goniometer, after unit cell indexing and crystal orientation determination

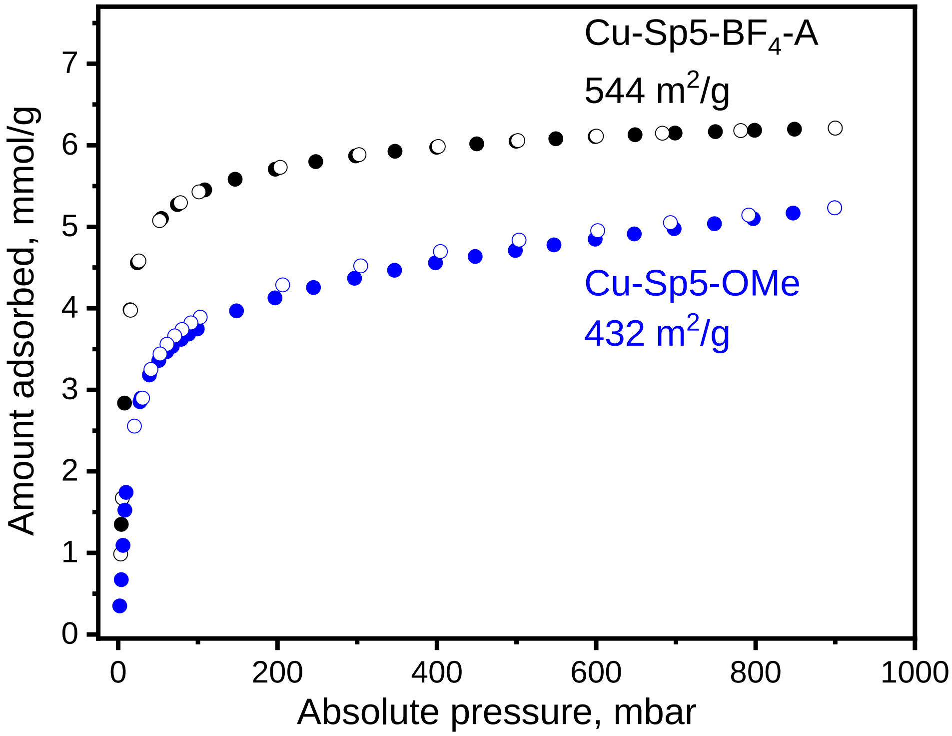

Figure S17. Gas adsorption isotherms (CO_2, 195K) of **Cu-Sp5-OMe** and **Cu-Sp5-BF4-A** and the corresponding Langmuir surface areas

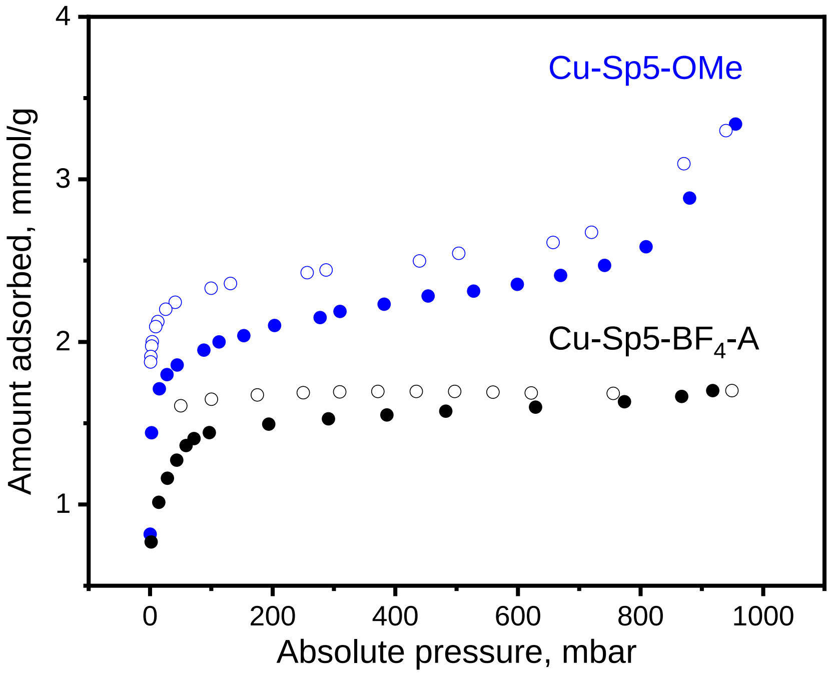

Figure S18. Gas adsorption isotherms (N_2, 77K) of **Cu-Sp5-OMe** and **Cu-Sp5-BF$_4$-A**

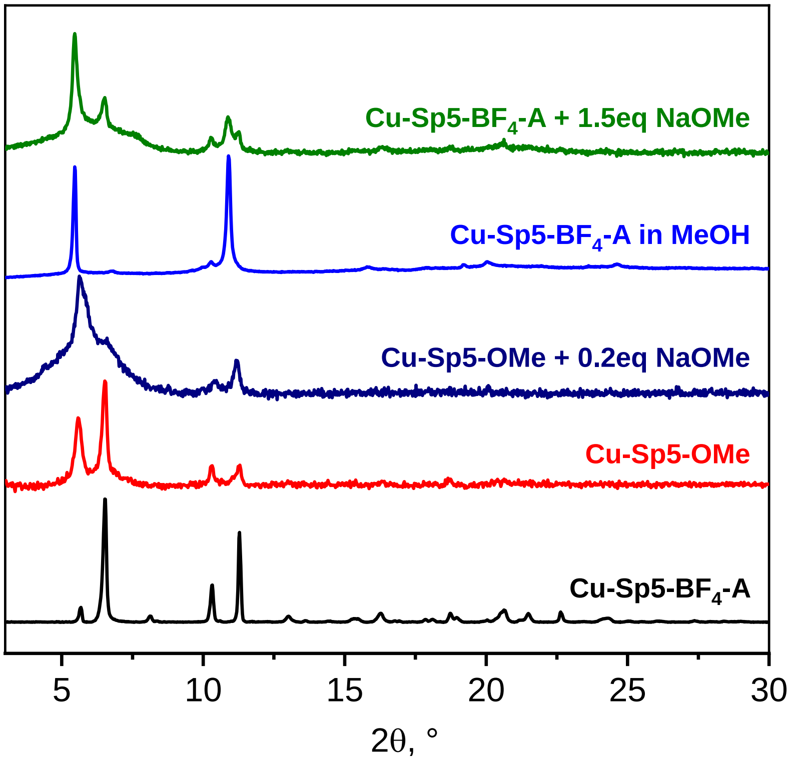

Figure S19. Powder diffraction patterns of materials obtained by treating **Cu-Sp5-OMe** and **Cu-Sp5-A** under different conditions.

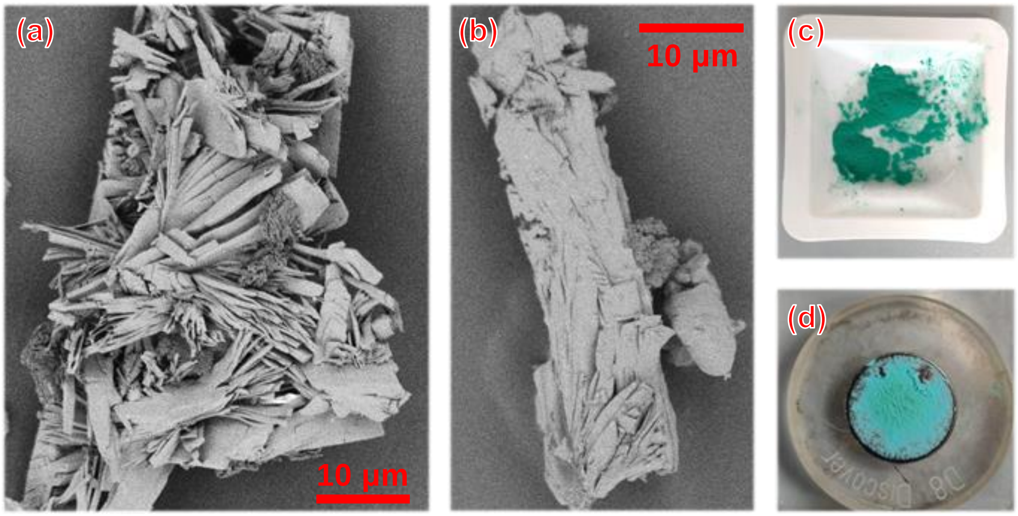

Figure S20. SEM images (a, b) and photos before (c) and after (d) air drying of **Cu-Sp5-BF$_4$-A** treated with MeOH for 24h

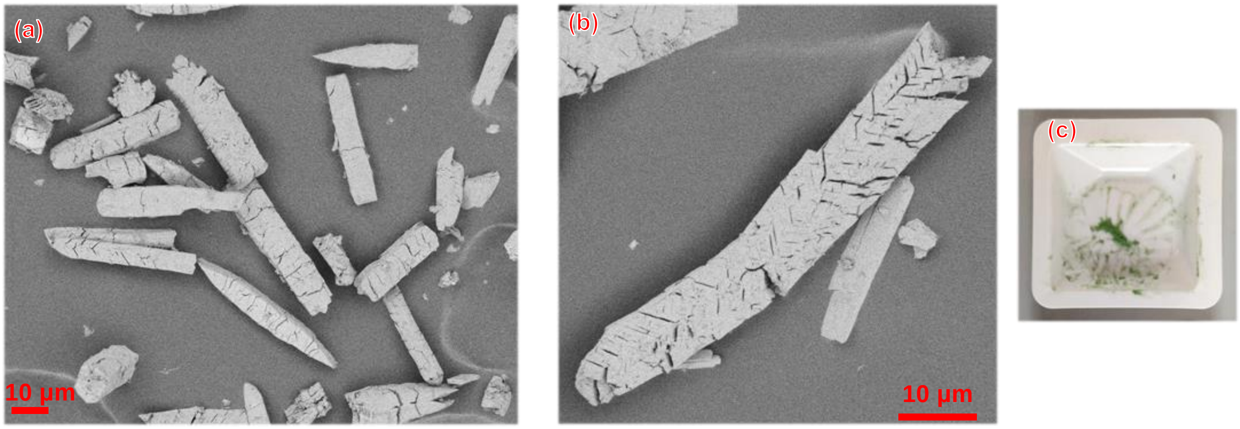

Figure S21. SEM images (a, b) and a photo (c) of **Cu-Sp5-BF$_4$-A** treated with 1.5 eq of NaOMe in MeOH for 24h

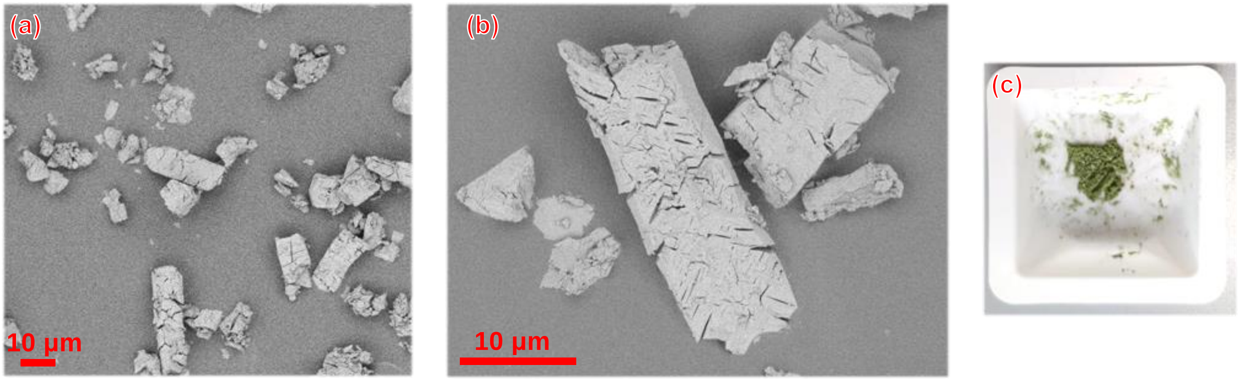

Figure S22. SEM images (a, b) and a photo (c) of **Cu-Sp5-OMe** treated with 0.2 eq of NaOMe in MeOH for 24h

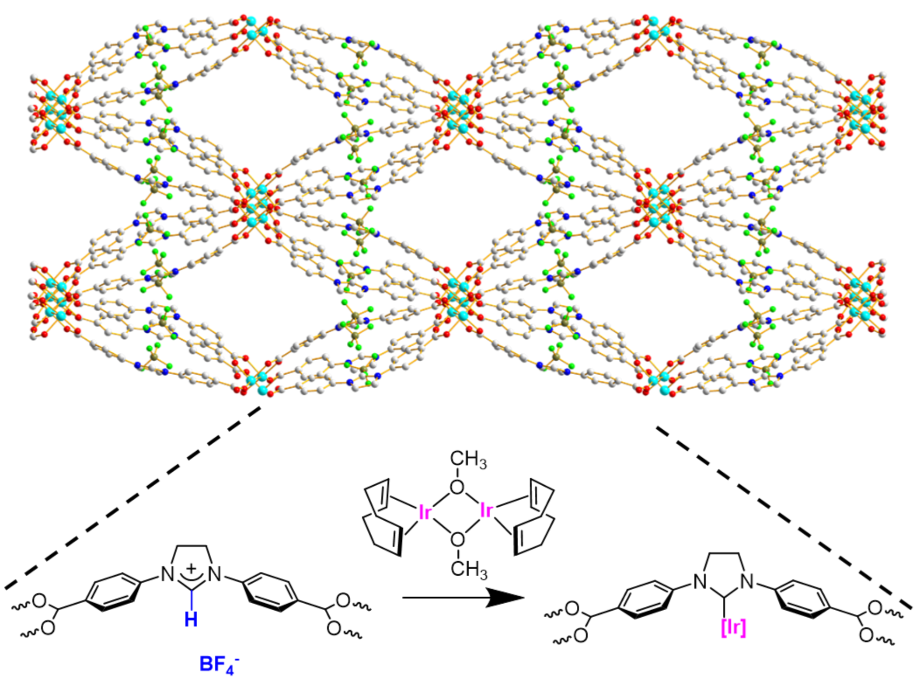

Scheme S1. Iridium modification on **Cu-Sp5-BF$_4$-A**

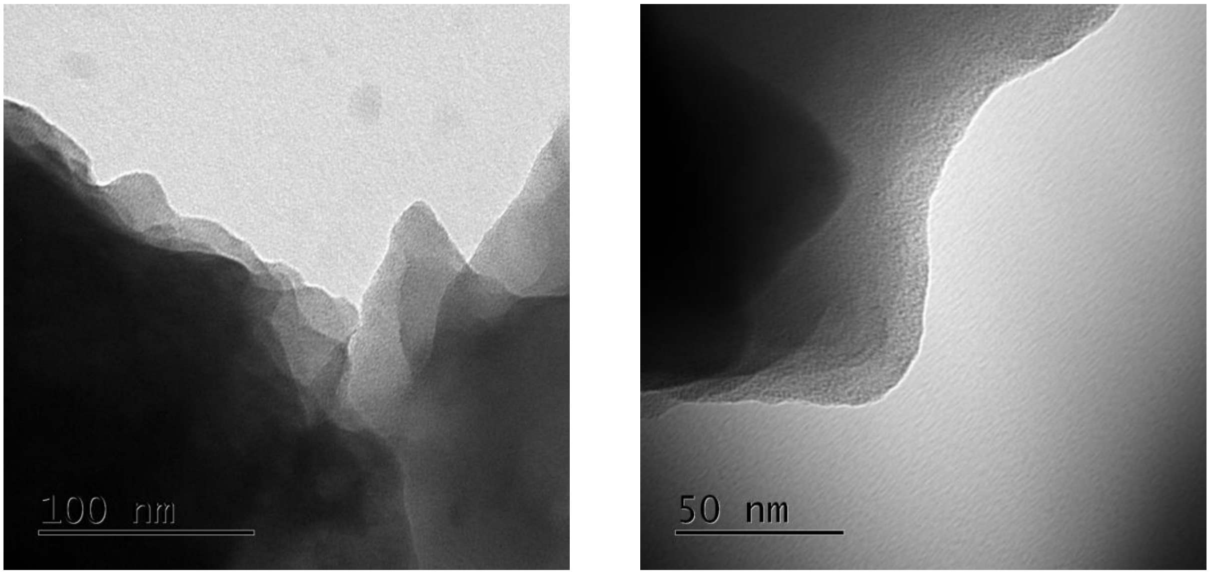

Figure S23. TEM images of **Ir**/**Cu-Sp5-OMe**

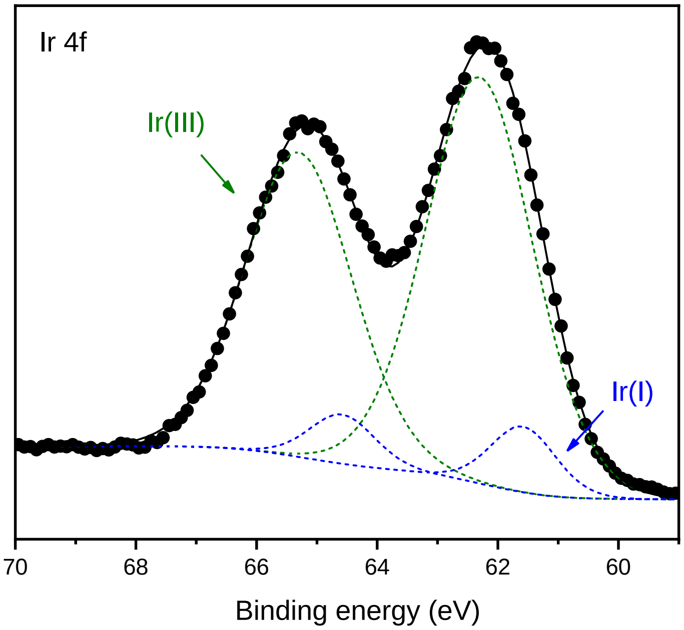

Figure S24. XPS spectrum of **Ir/Cu-Sp5-OMe**

Table S2. XPS fitting details for **Ir/Cu-Sp5-OMe**

	Ir(III) 7/2	Ir(III) 5/2	Ir(I) 7/2	Ir(I) 5/2
Peak energy (eV)	62.30	65.30	61.58	64.58
FWHM	2.11	2.11	1.27	1.27
Area (%)	52.07	39.04	5.08	3.81
Algorithm	Gauss/Lorentz	Gauss/Lorentz	Gauss/Lorentz	Gauss/Lorentz
Blend	0.3	0.3	0.3	0.3
Asymmetry	none	none	none	none

Table S3. Structures of complexes used for EXAFS fits and detailed information on the corresponding starting fit parameters

Entry #	**1**	**2**	**3**	**4**
Structure	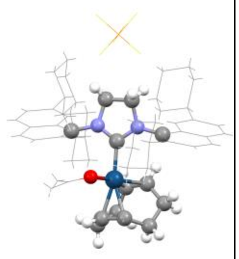	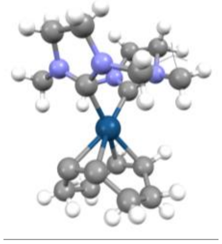	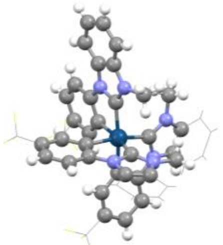	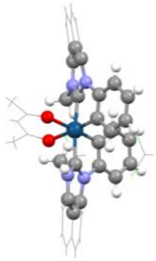
Name	**Mono-NHC-Ir(I)**	**Bis-NHC-Ir(I)**	**Tris-cyclometalated-Ir(III)**	**Bis-cyclometalated-Ir(III)**
Atom	C(NHC), C.N. 1, 2.06 Å	C(NHC), C.N. 2, 2.02 Å	C(NHC), C.N. 3, 2.03 Å	C(NHC), C.N. 2, 2.06
Atom 2	C(cod), C.N. 2, 2.11 Å	C(cod), C.N. 4, 2.11 Å	C(benzene), C.N. 3, 2.08 Å	C(benzene), C.N. 2, 1.99 Å
Atom 3	C(cod), C.N. 2, 2.20 Å	-	-	O(acac), C.N. 2, 2.17 Å
Atom 4	O(solvent), C.N. 1, 2.11 Å	-	-	-
CSD code	GARSAW	AZDCRH	KUNYAU	ASIHUG
Reference	[8]	[9]	[10]	[11]

Atom colors: Ir, dark blue; C, grey; O, red; N, blue; H, white. C.N. stands for Coordination Number

EXAFS fitting details for **Ir/Cu-Sp5-OMe** before catalysis:

Athena and Artemis software were used for the data analysis (background subtraction, normalization, etc.) of the Ir L-III edge XAS data and EXAFS fitting, respectively.[12] The amplitude reduction factor, S_0^2, was determined for the Ir metal reference ($S_0^2 = 0.70059$) and transferred to the sample to fit in order to reduce the number of refined parameters, while the coordination number (C.N.) was fixed to be the same for the three different atoms (C1, C2, O1). Iridium bis-cyclometalated complex model structure was taken from literature.[11, 13] ΔE_0 denotes the energy shift, ΔR_C and ΔR_O denote the adjustment in the half path length during the refinement for C and O atoms, respectively, and σ^2 denotes the Debye-Waller factor.

Goodness of fit parameters:

Reduced chi-square : 504.7882647

R-factor : 0.0184169

Fit results:

C.N. = 2.6 ± 0.3

$\Delta E_0 = 9.0 \pm 1.4$

$\Delta R\_C = 0.08 \pm 0.08$

$\Delta R\_O = -0.08 \pm 0.08$

$\sigma^2 = 0.004 \pm 0.002$

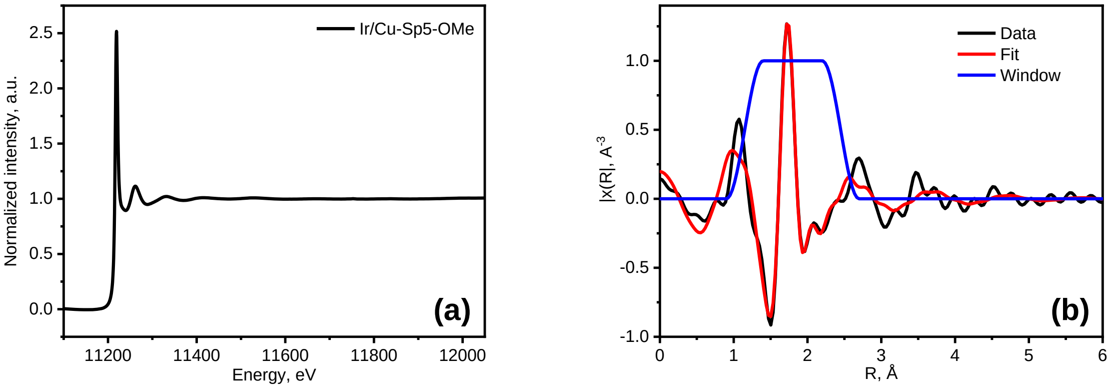

Figure S25. (a) Normalized EXAFS spectrum of **Ir/Cu-Sp5-OMe**, (b) Fitted EXAFS spectrum of **Ir/Cu-Sp5-OMe** in k-space

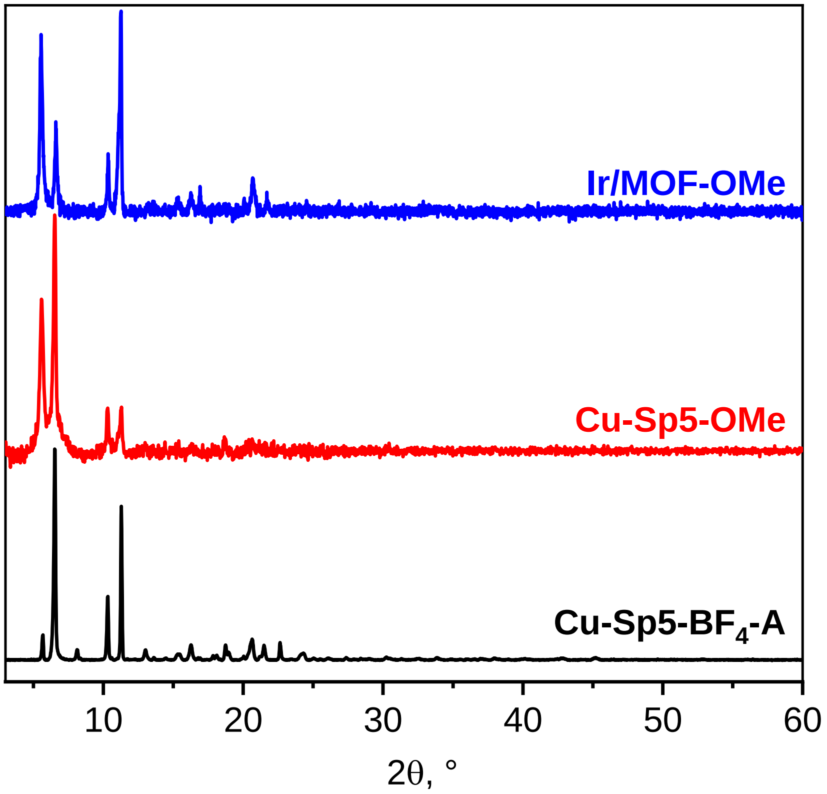

Figure S26. PXRD of **Ir/Cu-Sp5-OMe** compared to those of **Cu-Sp5-OMe** and **Cu-Sp5-BF$_4$-A**

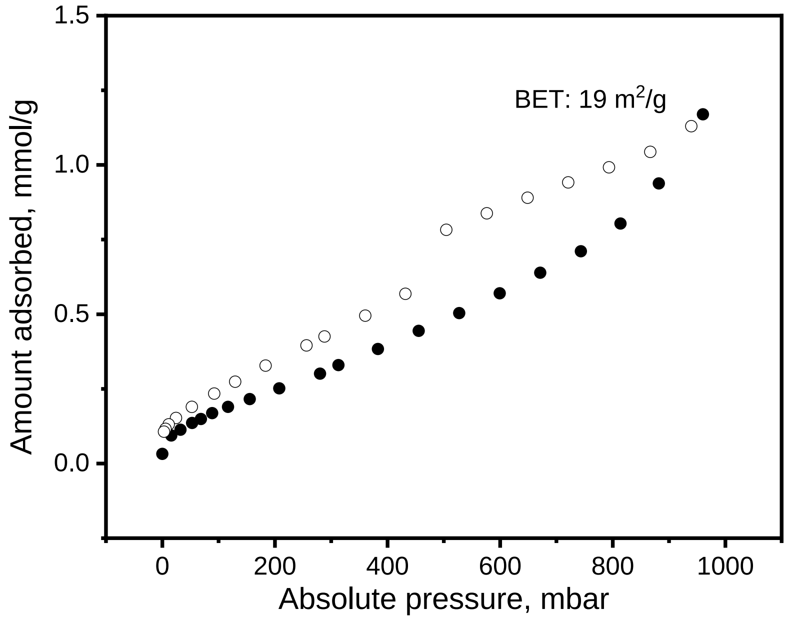

Figure S27. Gas adsorption isotherm (N_2, 77K) of **Ir/Cu-Sp5-OMe**

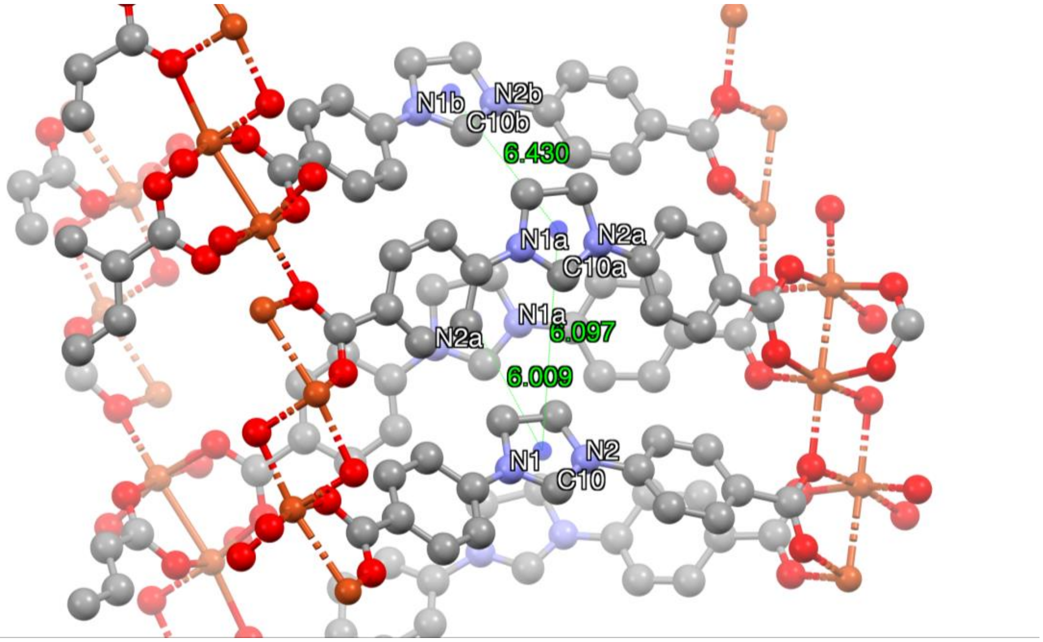

Figure S28. Distances between centers of neighboring NHC ligands in **Cu-Sp5-BF$_4$-A** structure. Hydrogen atoms and BF$_4^-$ ions are omitted for clarity. Atom colors: C, gray; O, red; N, blue; Cu, orange

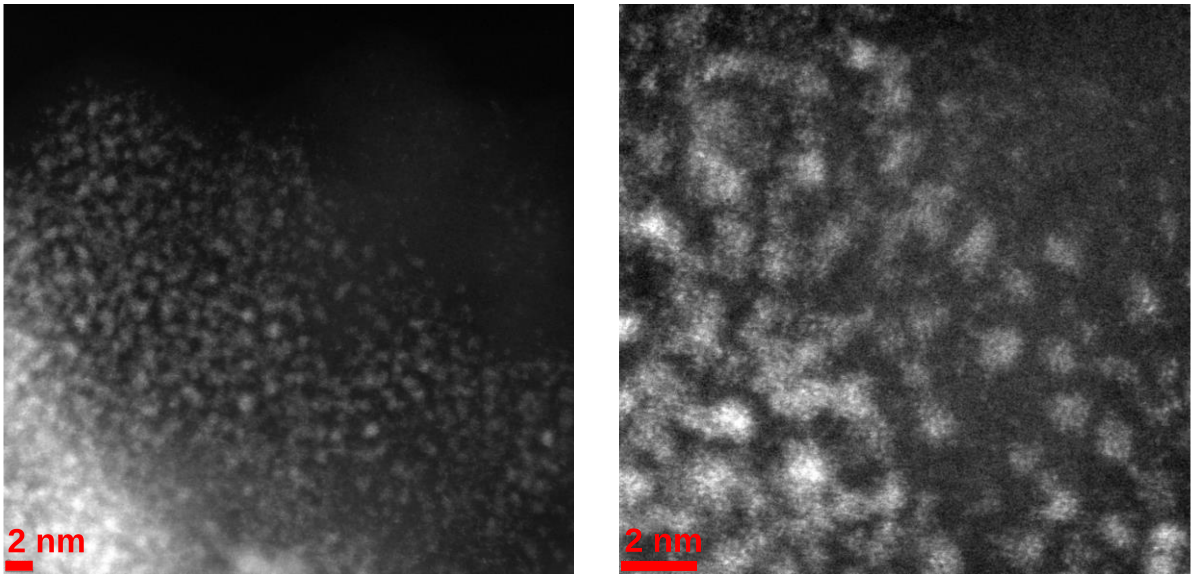

Figure S29. HAADF-STEM images of **Ir/Cu-Sp5-OMe**

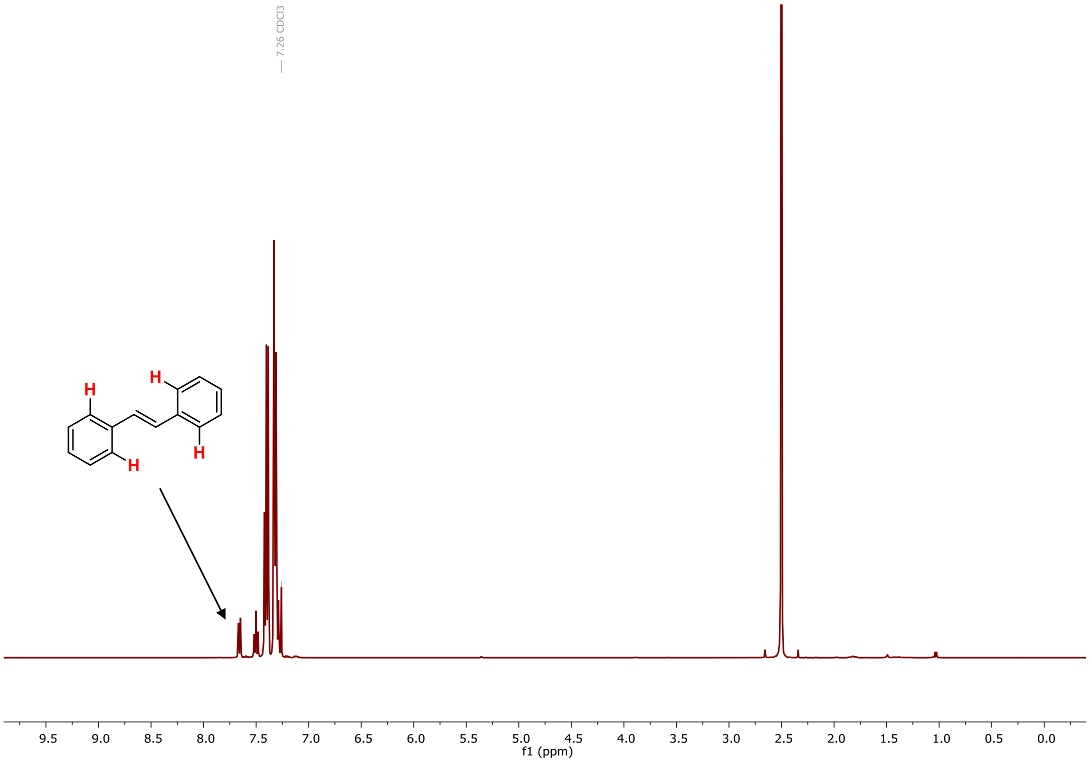

Figure S30. ^{1}H NMR ($CDCl_3$) spectrum of the solution after a catalytic run with a bare **Cu-Sp5-OMe** as a catalyst. No internal standard was used in this run.

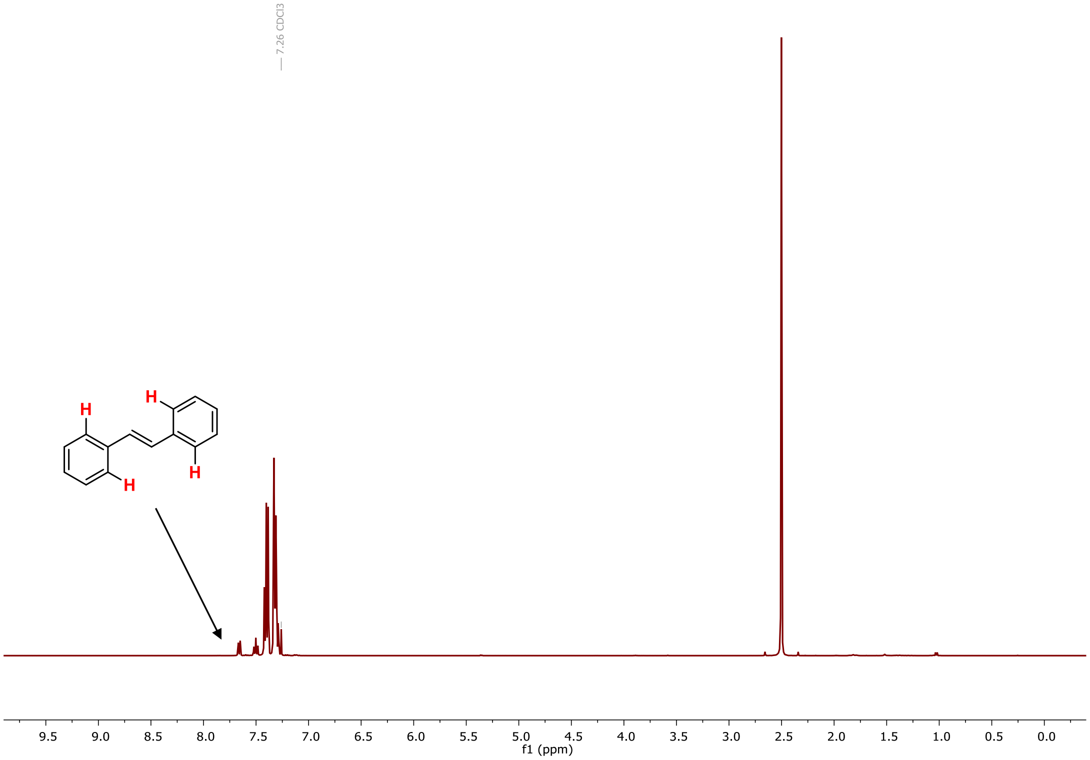

Figure S31. ^{1}H NMR ($CDCl_3$) spectrum of the solution after a catalytic run with a bare **Cu-Sp5-BF$_4$-A** as a catalyst. No internal standard was used in this run.

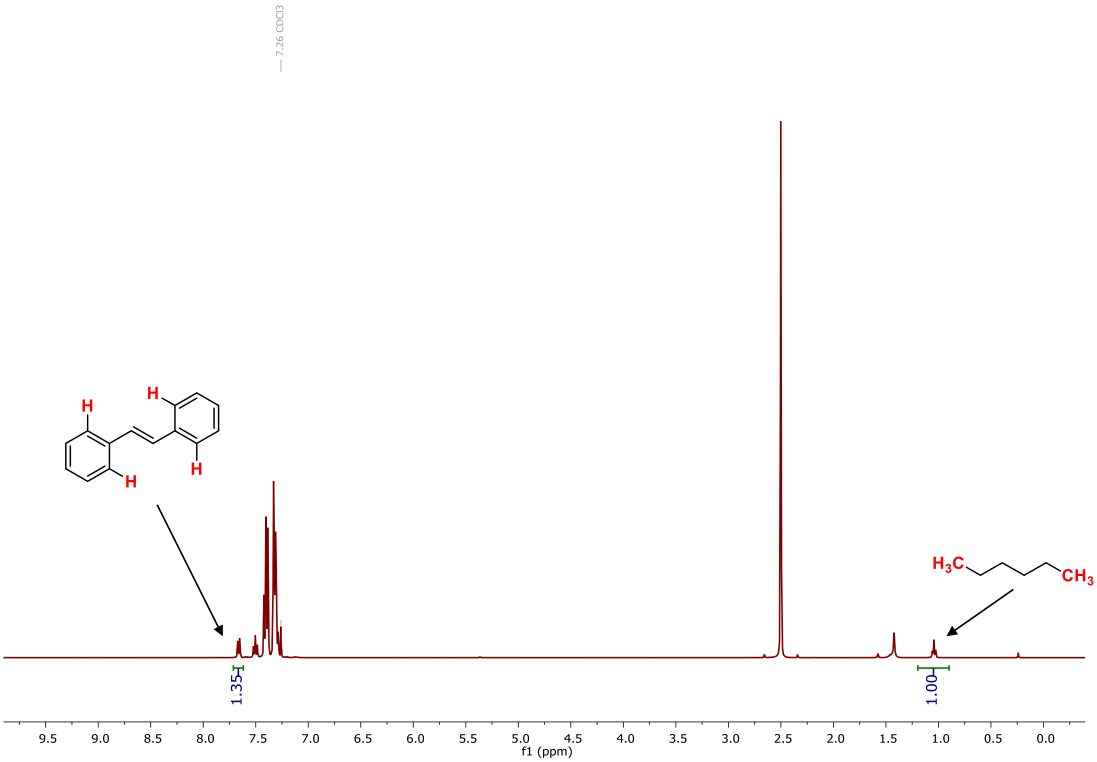

Figure S32. ${}^{1}H$ NMR ($CDCl_3$) spectrum of the starting material used for the Ir-catalyzed reactions (solution of trans-stilbene in toluene with n-hexane as an internal standard)

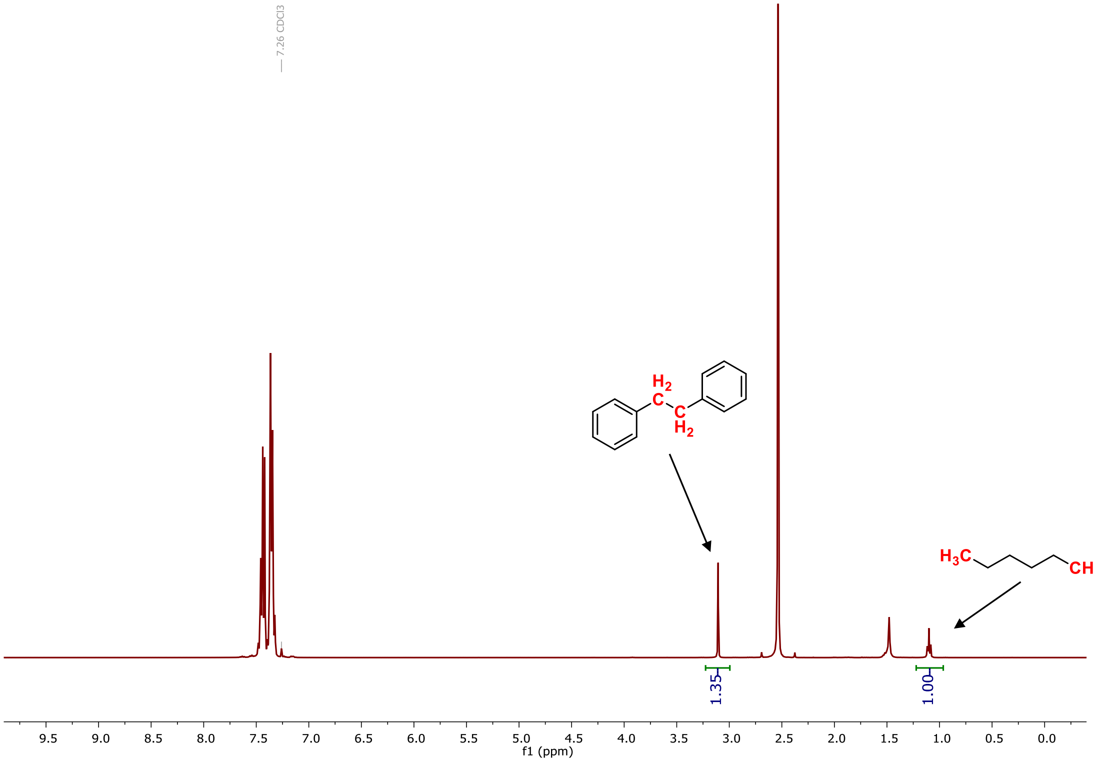

Figure S33. ${}^{1}H$ NMR ($CDCl_3$) spectrum of the solution after a catalytic run with a fresh **Ir/Cu-Sp5-OMe** catalyst

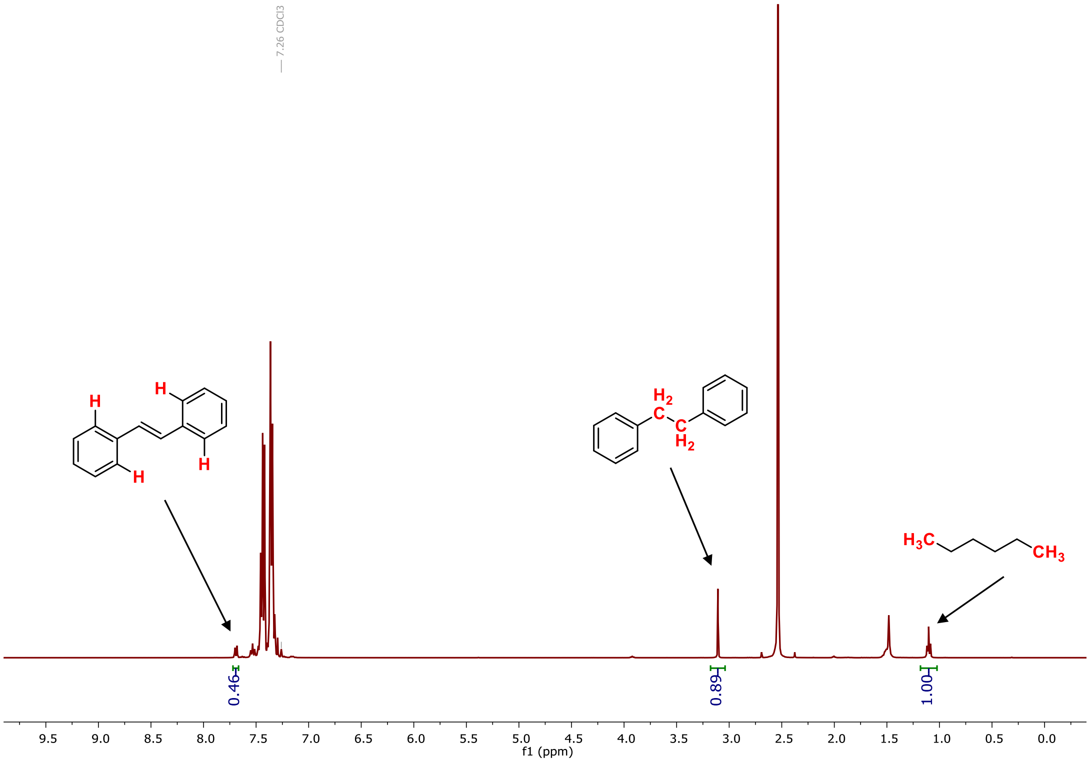

Figure S34. ^{1}H NMR ($CDCl_3$) spectrum of the solution after a catalytic run with a fresh **Ir/Cu-Sp5-BF₄-A** catalyst

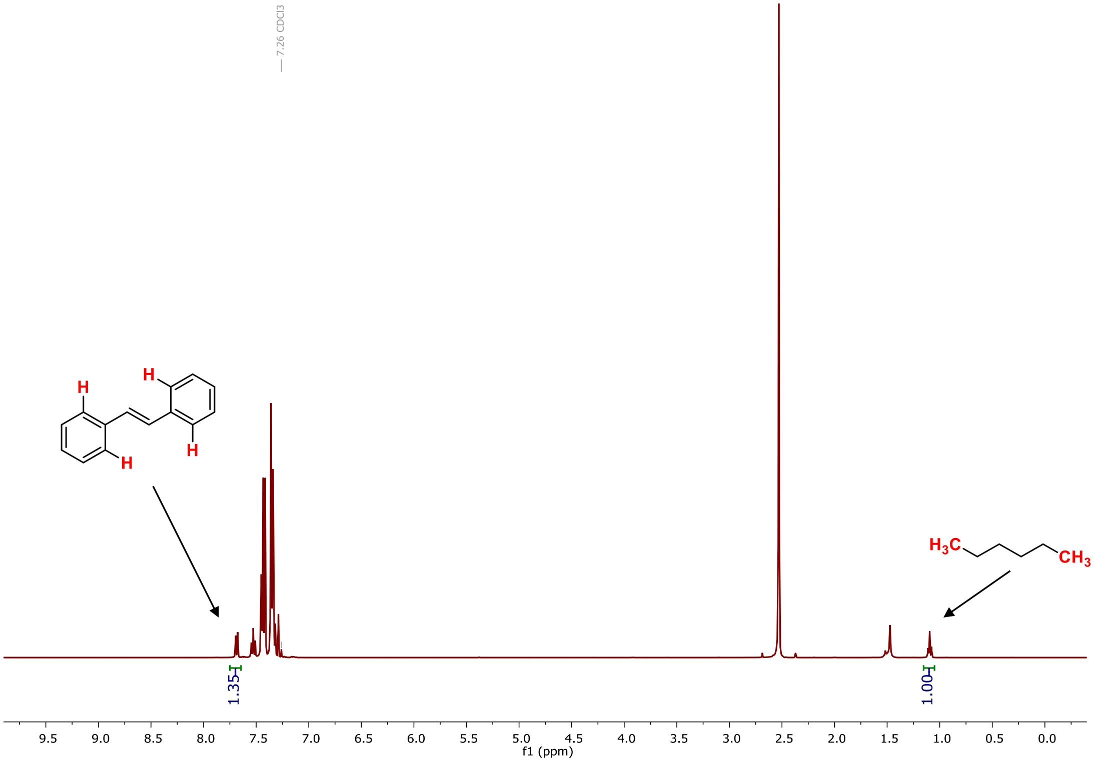

Figure S35. ^{1}H NMR ($CDCl_3$) spectrum of the solution after a catalytic run with a recycled **Ir/Cu-Sp5-OMe** catalyst

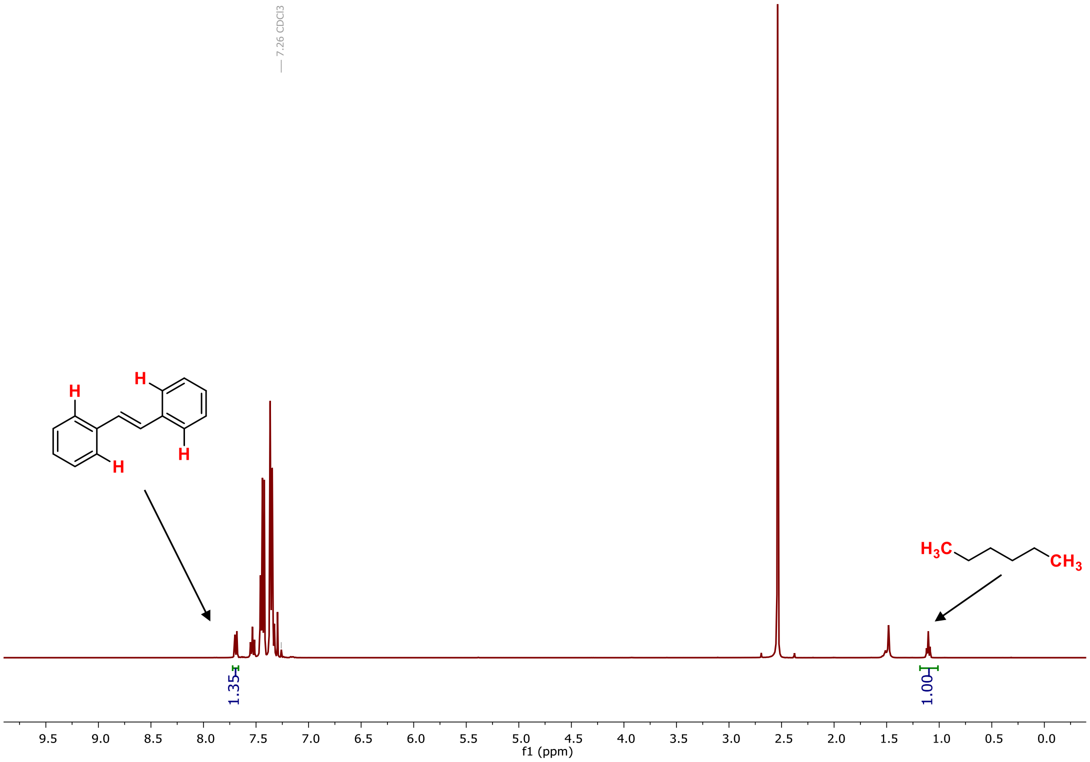

Figure S36. ^{1}H NMR ($CDCl_3$) spectrum of the solution after a catalytic run with a recycled **Ir/Cu-Sp5-BF4-A** catalyst

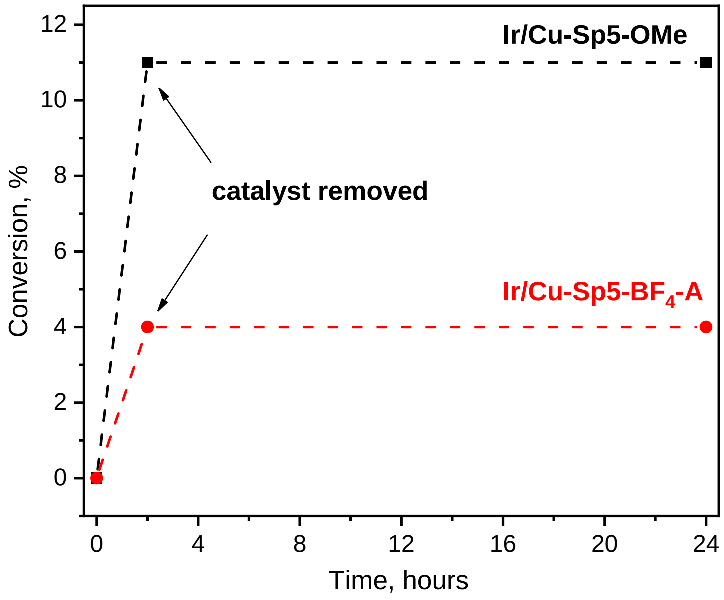

Figure S37. Catalyst separation test results for **Ir/Cu-Sp5-BF4-A** and **Ir/Cu-Sp5-OMe**

Table S4. Comparison of **Ir/Cu-Sp5-OMe** catalytic performance with reported supported Ir-NHC catalysts

Material	Substrate	Reaction parameters	Yield	Ref
Ir/Cu-Sp5-OMe	stilbene	5 bar H_2, 0.25 mol. % catalyst, 24h, 40 °C	>99%	This work
Ir-NHC grafted on silica	stilbene	3 bar H_2, 0.1 mol. % catalyst, 18 h, 40 °C	>99%	[14]
Ir-NHC grafted on MCM-41	diethyl 2-benzylidene succinate	4 bar H_2, 0.01 mol. % catalyst, 1 h, 40 °C	72.5	[15]
Ir-NHC grafted on MM clay	cyclohexene	1 bar H_2, 0.1 mol. % catalyst, 3.7 h, 17 °C	83	[16]

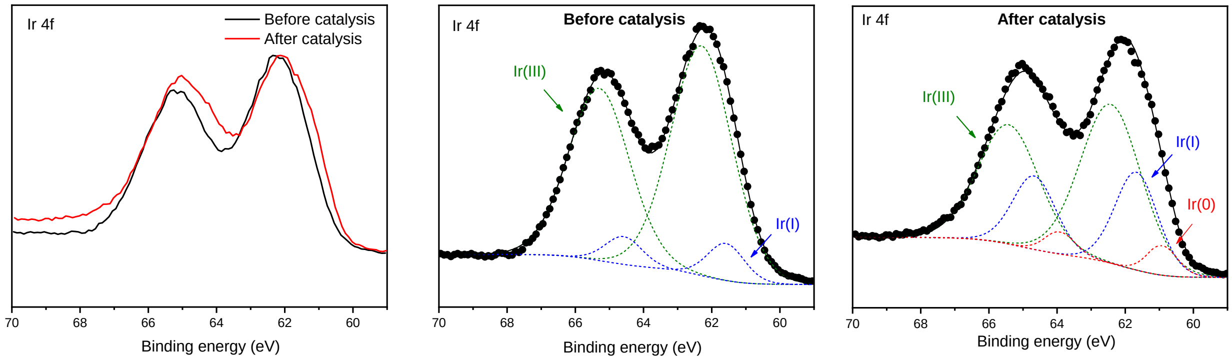

Figure S38. XPS spectra of **Ir/Cu-Sp5-OMe** before and after catalysis

Table S5. XPS fitting details for **Ir/Cu-Sp5-OMe** after catalysis

	Ir(III) 7/2	Ir(III) 5/2	Ir(I) 7/2	Ir(I) 5/2	Ir(0) 7/2	Ir(0) 5/2
Peak energy (eV)	62.422	65.422	61.670	64.670	60.900	63.900
FWHF	2.113	2.113	1.479	1.479	1.056	1.056
Area (%)	37.49	28.12	16.18	12.13	3.47	2.60
Algorithm	Gauss/Lorentz	Gauss/Lorentz	Gauss/Lorentz	Gauss/Lorentz	Asymmetric	Asymmetric
Blend	0.3	0.3	0.3	0.3	0.3	0.3
Asymmetry	none	none	none	none	0.5	0.5

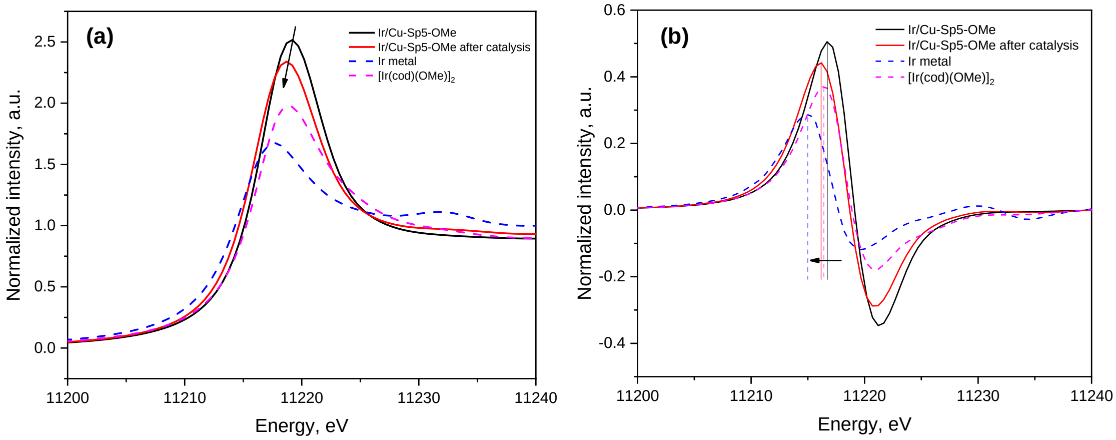

Figure S39. (a) XANES spectra of **Ir**/**Cu-Sp5-OMe** before and after catalysis (solid lines) and reference materials Ir metal and [Ir(cod)(OMe)]$_2$ (dashed lines). (b) First derivative of the spectra

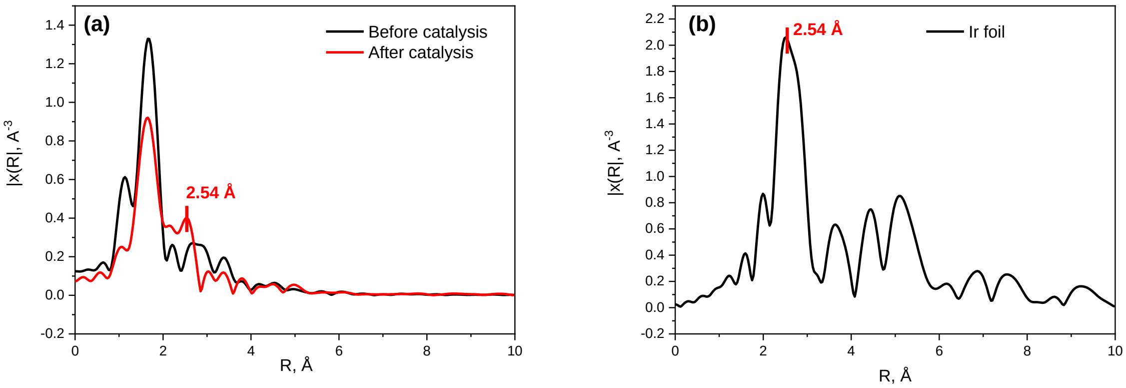

Figure S40. (a) R-space EXAFS spectra of **Ir**/**Cu-Sp5-OMe** before and after catalysis (b) R-space EXAFS spectrum of iridium foil.

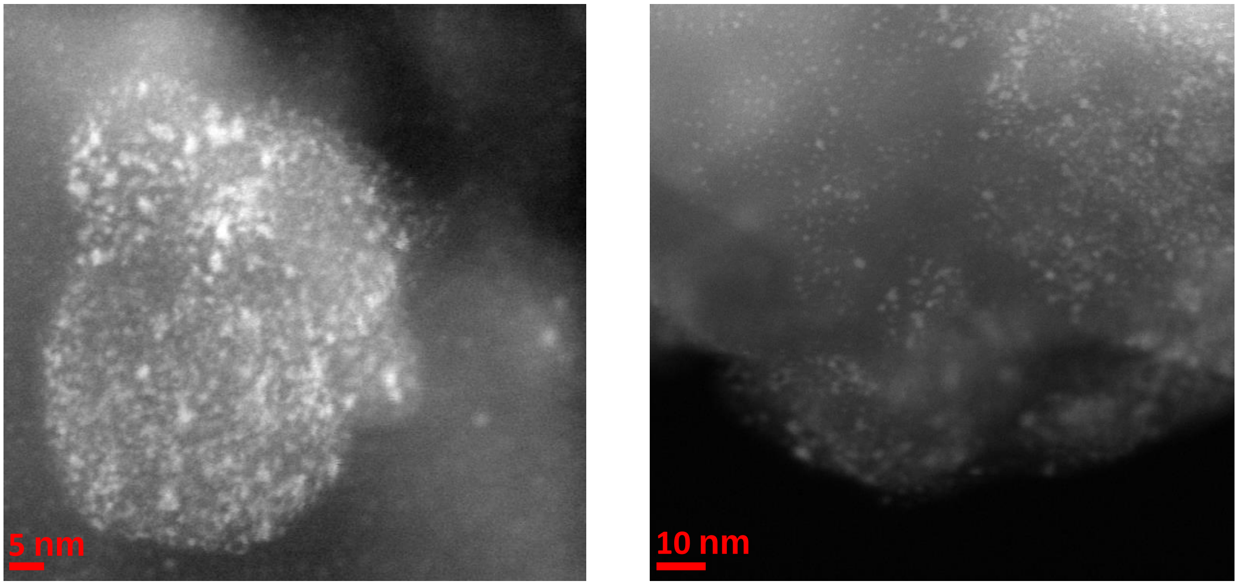

Figure S41. HAADF-STEM images of **Ir/Cu-Sp5-OMe** sample after catalytic cycle

References

1. *Bruker (2012). SAINT. Bruker AXS Inc., Madison, Wisconsin, USA.*
2. *Bruker (2001). SADABS. Bruker AXS Inc., Madison, Wisconsin, USA.*
3. G. M. Sheldrick, *Acta Crystallogr A Found Adv*, 2015, **71**, 3-8.
4. G. M. Sheldrick, *Acta Crystallogr C Struct Chem*, 2015, **71**, 3-8.
5. O. V. Dolomanov, L. J. Bourhis, R. J. Gildea, J. A. K. Howard and H. Puschmann, *Journal of Applied Crystallography*, 2009, **42**, 339-341.
6. D. Chernyshov, V. Dyadkin, W. van Beek and A. Urakawa, *Acta Crystallogr A Found Adv*, 2016, **72**, 500-506.
7. I. Kochetygov, S. Bulut, M. Asgari and W. L. Queen, *Dalton Trans*, 2018, **47**, 10527-10535.
8. G. Sipos, P. Gao, D. Foster, B. W. Skelton, A. N. Sobolev and R. Dorta, *Organometallics*, 2017, **36**, 801-817.
9. P. B. Hitchcock, M. F. Lappert, P. Terreros and K. P. Wainwright, *Journal of the Chemical Society, Chemical Communications*, 1980, DOI: 10.1039/C39800001180, 1180-1181.
10. K. Tsuchiya, S. Yagai, A. Kitamura, T. Karatsu, K. Endo, J. Mizukami, S. Akiyama and M. Yabe, *European Journal of Inorganic Chemistry*, 2010, **2010**, 926-933.
11. H. Tsurugi, S. Fujita, G. Choi, T. Yamagata, S. Ito, H. Miyasaka and K. Mashima, *Organometallics*, 2010, **29**, 4120-4129.
12. B. Ravel and M. Newville, *Journal of Synchrotron Radiation*, 2005, **12**, 537-541.
13. Y. Zhou, J. Jia, W. Li, H. Fei and M. Zhou, *Chemical Communications*, 2013, **49**, 3230-3232.
14. I. Romanenko, D. Gajan, R. Sayah, D. Crozet, E. Jeanneau, C. Lucas, L. Leroux, L. Veyre, A. Lesage, L. Emsley, E. Lacote and C. Thieuleux, *Angew Chem Int Ed Engl*, 2015, **54**, 12937-12941.
15. C. González-Arellano, A. Corma, M. Iglesias and F. Sánchez, *Inorganica Chimica Acta*, 2004, **357**, 3071-3078.
16. M. Crocket and R. H. M. Herold, *Catal Lett*, 1993, **18**, 243-251.